Hydrogen isotopic composition of CI- and CM-like clasts from meteorite breccias - sampling unknown sources of carbonaceous chondrite materials

Markus Patzek*[1], Peter Hoppe[2], Addi Bischoff[1], Robbin Visser[3], and Timm John[3]

* Corresponding author

[1]Institut für Planetologie, Westfälische Wilhelms-Universität Münster, Wilhelm-Klemm-Str. 10, D-48149 Münster, Germany

[2]Max Planck Institute for Chemistry, Particle Chemistry Department, P.O. Box 3060, D-55020 Mainz, Germany

[3]Freie Universität Berlin, Institut für Geologische Wissenschaften, Malteserstr. 74-100, D-12249 Berlin

Reviewed version 6th of December

Abstract

Volatile-rich, CI- and CM-like clasts occur in different brecciated achondrite and chondrite groups. The CI-like clasts in HEDs, polymict ureilites, as well as ordinary, CR, and CB chondrites have a similar mineralogy, indicating a similar alteration history. However, when viewed in detail, their mineral chemistry shows some minor differences between the clasts from different meteorite groups. For CM-like clasts found in HED meteorites, the clasts are, based on their mineralogy, clearly fragments of CM chondrites. To be able to decipher whether CI- (or CM-)like clasts from different meteorite groups are related to certain meteorite classes known to contain volatiles, we obtained D/H ratios of several clasts from the meteorite groups mentioned above and compared them with those of CI and CM chondrites as well as to unique carbonaceous chondrites such as Bells, Essebi, and Tagish Lake. Considering the δD-values, CM-like clasts in HEDs span a similar range compared to bulk values of CM chondrites, further indicating that CM-like clasts are fragments of CM chondrites. For CI-like clasts a clear distinction can be made: While CI-like clasts in HEDs and ordinary chondrites show a very similar range in their δD-signatures compared to "common" CI chondrites, meaning that these clasts are likely related to CI chondrites, the CI-like clasts in polymict ureilites are enriched in D up to 3000 ‰; a similarly high enrichment is found for the CI-like clasts in CR chondrites. Thus, although the CI-like clasts in ureilites and CR chondrites likely experienced similar alteration histories as the CI-like clasts found in the other meteorite types, these clasts probably formed in a different region than the CI chondrites and, thus, are more accurately referred to as C1 clasts. Overall, the existence and isotopic signatures of the C1 clasts in several meteorite groups proves the existence of additional primitive, volatile-rich material in the (early) Solar System besides the matter we study as the CI, CM, and CR chondrites. This material was distributed throughout the Solar System very early and might have played an important role for the volatile inventory of the terrestrial planets.

1. Introduction

Meteoritic breccias give us the possibility to study processes and relative timings of different events in their history and possible relationships between different parent bodies (e.g., Bischoff et al., 2006). Xenolithic clasts, which are not represented in the current sample collection as individual meteorites, are of special importance. Numerous studies have shown that xenolithic carbonaceous chondrite material is present in many different chondrites and volatile-poor achondrites such as ureilites and HED meteorites. When we refer to “xenolithic carbonaceous material” in this work, we do not mean dark inclusions as those found in Allende or in other meteorite samples (e.g., Bischoff et al., 1988; 2006), but instead are referring to volatile-rich clasts consisting of abundant water-bearing phases and minerals precipitated from aqueous fluids (e.g., carbonates, magnetites, sulfates, pyrrhotite).

Based on chemical, mineralogical and textural criteria, these clasts have been correlated to known groups of carbonaceous meteorites or they have been grouped by their optical characteristics; thereby, researchers have identified both CI-like and CM-like clasts (e.g., Zolensky et al., 1996; Gounelle et al., 2005, Patzek et al., 2018a). Due to the high abundance of CM-like material in HEDs, extensive work has been carried out on breccias of these meteorites, and results show a clear trend in that CM-like clasts are related to CM and CR chondrites (Zolensky et al., 1996). Nonetheless, many researchers have indicated that this volatile-rich carbonaceous chondrite material differs in some aspects from “common” carbonaceous chondrite groups (Zolensky et al., 1996; Briani et al., 2012). Further, volatile-rich clasts are also found in carbonaceous chondrites themselves, e.g. CR and CH chondrites (Grossman et al., 1988; Scott, 1988; Weisberg et al., 1988; Endress et al., 1994; Bischoff et al., 1993a, b), CM chondrites and Tagish Lake (C2) (Zolensky et al., 2015; 2017).

Consequently, various studies have aimed to further decipher the origin of these CM-like and CI-like volatile-rich clasts. For example, based on a study of carbonaceous clasts in howardites and H chondrites, Gounelle et al. (2003, 2005) point out a possible zodiacal origin for volatile-rich clasts as fossil micrometeorites. They also provide data on the hydrogen isotopic composition of these hydrous, volatile-rich clasts, whereby they found that the range in D/H ratio of the hydrous clasts in howardites is similar to that found for Antarctic micrometeorites. Thus, Gounelle et al. (2005) refer to these clasts as fossil micrometeorites trapped in the early Solar System.

As similar volatile-rich, hydrous clasts are also found in other chondrite and achondrite groups (e.g. CH, CB, CR, ureilites, OC and R chondrites) their distribution might provide insights into the formation process of the brecciated meteorite carrying these clasts (polymict ureilites: Prinz et al., 1987; Brearley and Prinz, 1992; Brearley and Jones, 1998, Goodrich and Keil, 2002; Ikeda et al., 2003; Goodrich et al., 2004; in CR chondrites: Bischoff et al.,1993a; Endress et al., 1994; in CH chondrites: Bischoff et al., 1993b; in R chondrites: Greshake, 2014; in H chondrites: Funk et al., 2011; Briani et al., 2012; Zolensky et al., 2016; Bischoff et al., 2018). Since these clasts are so similar to each other in their mineralogy, we explore similarities and possible links between the clasts themselves and between the clasts and other meteorite types by determining the D/H ratios of CI- and CM-like clasts from different meteorites and compare these ratios to those found for "common" aqueously-altered carbonaceous chondrites. This approach allows us to discuss and subdivide the CI-like clasts found in different chondrites and achondrites and speculate on their origin. Additionally, we evaluate whether all CI-like clasts are really similar to CI1 (Ivuna)-type chondrites of petrologic type 1 or whether these clasts are better referred to as C1 clasts. Preliminary results of this work were published in a conference abstract by Patzek et al. (2017) and recent work aiming at the $\delta^{34}S$ signature of sulfides within CI-like clasts from different host rocks and CI chondrites indicate that they incorporated isotopically distinct sulfur (Visser et al., 2019).

2. Analytical techniques

Volatile-rich clasts in polished thin sections can be easily identified in reflected light in chondrites and achondrites due to their high modal abundance of fine-grained phyllosilicates, which have a distinct texture compared to anhydrous minerals such as olivine and pyroxene. We selected the clast-containing samples to be used in this study based on a survey performed in a previous work, which describes details on the clasts' abundance, size, and mineralogy (Patzek et al., 2018a).

We determined the D/H ratios together with C/H, Si/H, and CN/H (see appendix) ratios of several clasts and samples using a Cameca NanoSIMS 50 ion probe at the Max Planck Institute for Chemistry in Mainz (Hoppe et al., 2013). Special care was taken for selecting appropriate areas representative for clasts. These areas are free of cracks, chondrules, CAIs, larger olivine and pyroxene grains, as well as areas indicating a terrestrial deposition of iron hydroxides. Prior to the isotope measurements, the samples were cleaned for 30 min in an ultrasonic bath with ethanol, and heated for ~3h at ~80 °C in the NanoSIMS airlock at starting pressures of $p < 10^{-6}$ Torr to remove adsorbed water. Phyllosilicate-rich areas in volatile-rich clasts (list of samples and total analyzed areas in Table 1) were selected based on the previously mentioned characteristics, and 20 x 20 µm² to 25 x 25 µm²-sized fields were pre-sputtered with a high-current Cs^+ beam (120-730 pA) for up to 55 minutes to remove the carbon coating and surface contamination. We acquired negative secondary ion images (20 x 20 µm², 256 x 256 pixels) in a combined peak switching (two magnetic fields) and multi-collection mode (magnetic field 1: H, D; magnetic field 2: ^{12}C, $^{12}C^{14}N$, ^{28}Si), employing a primary Cs^+ beam (4 pA, ~200 nm). Each measurement consisted of five image planes with integration times of 3000 µs/pixel/plane for H and D, and 1000 µs/pixel/plane for ^{12}C, $^{12}C^{14}N$, and ^{28}Si. No electron gun was required for charge compensation since no significant charging was observed during any of the analyses. Results are given in standard delta notation ($\delta D = [(D/H)_{sample}/(D/H)_{std} - 1] \times 1000$) using the terrestrial VSMOW value of D/H=155.76 x 10^{-6} as reference. Ilimaussaq Amphibole (δD_{VSMOW} = -142 ‰) and synthetic $C_{30}H_{50}O$ (δD_{VSMOW} = -151 ‰; kindly provided by Erik Hauri and Larry Nittler, Carnegie Institution, Washington D. C.) were used as isotope standards to determine the instrumental mass fractionation (IMF) for D/H measurements. On average, the IMF was determined as -280 ‰ for $C_{30}H_{50}O$ and -230 ‰ for Ilimaussaq Amphibole. Hydrogen in clasts is a mixture of H in phyllosilicates and H bound in organics. The similar IMF values for our standards, which have completely different chemical composition, seem to indicate that matrix effects on measured D/H ratios are relatively small in the analytical setup chosen for this study. This is also supported by the good agreement of our measurements of matrix material in Ivuna, Essebi, Bells, and Tagish Lake with respective bulk data from the literature (see section 4). We used the IMF inferred from measurements on our $C_{30}H_{50}O$ standard to correct the measured D^-/H^- ratios in clasts. Piani et al. (2012) and Remusat et al. (2016) found that for samples of meteoritic insoluble organic matter (IOM), which are strongly enriched in D, D^-/H^- ratios measured on the NanoSIMS are about 50% lower than the D/H ratios determined by gas mass spectrometry. This is unlikely to be solely IMF but was interpreted to be also the result of contamination with terrestrial H, adsorbed, e.g., from the residual gas in the analysis chamber of the NanoSIMS, which may in principle also affect the different H reservoirs in meteoritic thin sections to some extent. However, even if contributions of H contamination cannot be fully excluded in our work, the similarities in D/H ratios obtained in our work for CI and C2 chondrites, having δD values of up to several 100 ‰ (see section 4), with that of bulk values measured by gas mass spectrometry show that our approach and tuning provide valid and reproducible results. This permits us to draw at least qualitative conclusions on the H-isotopic signatures of CI- and CM-like clasts compared to those of bulk carbonaceous chondrites. Errors reported here are 1σ and are based on counting statistics and include the reproducibility of D/H ratios measured for the $C_{30}H_{50}O$ standard (10 to 25 ‰, depending on the measurement session). Presented averages of isotope/elemental ratios are weighted averages, calculated by adding the number of counts of individual spots over their total area. Errors of averages are given in the following discussion as the (unweighted) standard deviation of the mean (line "sd" in Table 3), which better reflects heterogeneities than the standard error of weighted averages (column “1σ” in Table 3). Relative sensitivity factors needed to calculate atomic C/H and Si/H ratios from measured $^{12}C^-/H^-$ and $^{28}Si^-/H^-$ ratios were determined from Ilimaussaq Amphibole (Si/H) and synthetic $C_{30}H_{50}O$ (C/H). Elemental ratios may be strongly affected by matrix effects, and uncertainties of inferred C/H and Si/H ratios are estimated to be at least a factor of two. This should be considered when the inferred C/H and Si/H ratios are compared with respective data for bulk chondrites from literature. Based on measured D/H vs. C/H ratios of epoxy in this study (C/H = 0.4, $\delta D = -250 \pm 10$ ‰) significant contributions to our measurements of meteoritic matter appear unlikely. The H background from the NanoSIMS can have noticeable effects on the D/H ratio if the concentration of hydrogen in the sample is low. For samples analyzed in this study, however, the abundance of hydrogen in clasts is more than an order of magnitude higher than the upper limit on the H background in the NanoSIMS, inferred from a measurement on a Si-wafer.

3. Mineralogy and mineral chemistry

Based on previous investigations of the mineralogy (Patzek et al., 2018a) two major groups of volatile-rich clasts have been identified (1) CM-like clasts and (2) CI-like clasts. Below some basic characteristics will be described (for more information, see Patzek et al., 2018a). Since Tagish Lake, Bells, and Essebi contain lithologies similarly rich in magnetite when compared to CI-like clasts and CI chondrites, some basic data on the mineralogy of the carbonaceous chondrites Bells, Essebi, Tagish Lake and Ivuna are given. For a summary see Table 2. Previous work using Raman thermometry implies only minor heating of these clasts. Peak temperatures experienced by CI-like clasts range between 30–110 °C with an average of about 65 ± 25 °C, and the peak temperatures experienced by CM-like clasts range from 50 to 110 °C with an average of about 70 ± 25 °C (Visser et al., 2018).
The organic chemistry of carbonaceous chondrites in general - in particular those of aqueously altered chondrites - is very complex. Organic molecules are often enriched in D and occur as aggregates of different “grain” sizes ranging from nanometers to some micrometers (Alexander et al., 2010, 2012, 2017; Le Guillou et al., 2014, and references therein). The investigation of these organic grains is complex and usually requires the resolution offered by transmission electron microscopy. Nonetheless, the organics have important implications for the data obtained in this study and will be discussed in a separate section (5.1).

3.1. CM-like clasts

The typical mineralogy of CM-like clasts includes varying amounts of tochilinite-cronstedtite-intergrowth (TCI) clumps with a wavy texture, abundant chondrules and fragments of anhydrous minerals (Fig. 1; Johnson and Prinz, 1993; Zolensky et al., 1997; Rubin et al., 2007). The TCIs as well as the anhydrous minerals are often surrounded by fine-grained rims, which are described as accretionary dust rims (Metzler et al., 1992). Occasionally, Fe,Ni-metal grains can be observed within chondrules but are not directly embedded within the hydrous matrix phyllosilicates. Sulfides are abundant and occur as irregularly-shaped grains of pyrrhotite and pentlandite. Carbonates occur in CM-like clasts and are mostly pure calcite/aragonite. The carbonate grains are irregularly-shaped and do not show any incipient secondary alteration. All components are embedded into a clastic matrix consisting of fine-grained phyllosilicates and TCI clumps. The mesostasis within chondrules has been altered to phyllosilicates. We analyzed areas dominated by TCI clumps, matrix-dominated areas, and areas representing a mixture of these two mineralogically different components.

3.2. CI-like clasts

CI-like clasts are phyllosilicate-rich clasts containing magnetite, sulfides and occasionally accessory phases such as carbonates, phosphate, and chromites. Chondrules and fragments of anhydrous silicates (mostly forsteritic olivine) are rare and – if present – always irregularly-shaped. The magnetite grains occur either as irregularly-shaped grains, as framboids, as isolated spherical magnetite, or as plaquettes (Fig. 2; and Fig. 6 in Patzek et al., 2018a). Sulfides are common and include pyrrhotite of different composition and pentlandite. Pentlandite grains occur as irregularly-shaped grains, whereas pyrrhotite exhibits lath-shaped as well as irregularly-shaped grains. The pyrrhotite composition varies between $Fe_{0.85}S$ and stoichiometric FeS, but pyrrhotite grains often contain exsolution blobs and lamellae (<1 µm) of a Ni-rich phase (probably pentlandite). Accessory phases include carbonates and phosphates. The fine-grained matrix is texturally highly heterogeneous with embedded sub-µm sized grains of Fe sulfides and/or oxides (Figs. 2 b,d,f) and yields low analytical totals of 80-90 wt% confirming the presence of volatile components (e.g., H_2O) and/or microporosity. See Patzek et al. (2018a) for the bulk composition of the clasts and their matrices. In some volatile-rich clasts, homogeneous patches of phyllosilicates can be observed, which are free of any fine-grained oxides or sulfides but clearly show a fibrous texture reflecting pseudomorphic replacements of former olivine or pyroxene grains by phyllosilicates. Rare chondrules with maximum diameters of 150 µm have only been found in a small number of CI-like clasts from polymict ureilites and CR chondrites but not in those from other host meteorites.

3.3. Al Rais and Renazzo

Al Rais is a somewhat special CR2 chondrite, and it is known for its high abundance of dark inclusions (Weisberg et al., 1993). These dark inclusions have a similar mineralogy compared to CR chondrite matrix portions, and their formation processes are subject to discussion (Weisberg et al., 1993; Endress et al., 1994; Patzek et al., 2018a). Their mineralogy is similar to those of CI-like clasts in other meteorite groups. A variety of different fragments with different alteration stages can be found right next to each other. In general, Al Rais shows a higher degree of aqueous alteration and a higher abundance of CI-like clasts than other CR chondrites such as Renazzo. Renazzo, however, does contain abundant CI-like clasts similar to those in Al Rais.

3.4. Ivuna, Bells, Essebi, and Tagish Lake

The typical mineralogy of CI chondrites such as Ivuna includes magnetite spherules, framboids, plaquettes or irregularly-shaped grains, all of which are embedded within a phyllosilicate-rich matrix. The phyllosilicates are a fine-grained mixture of saponite and serpentine minerals. Lath-shaped pyrrhotite grains with varying composition ($Fe_{1-X}S$), carbonates of different composition as well as phosphates can be abundant (compare Endress and Bischoff, 1996). However, CI chondrites are brecciated rocks consisting of different lithologies having a slightly different mineralogy on the scale of 50 to several 100 µm (compare Morlok et al., 2006). Mafic silicates such as olivine or pyroxene are rare.

The mineralogy of the ungrouped C2 chondrite Bells includes varying abundances of chondrules occasionally surrounded by fine-grained rims similar to those found within CM2 chondrites (Metzler et al., 1992). Compared to CM chondrites, the abundance of magnetite is significantly higher and similar to some lithologies in CI chondrites. Fragments of olivine and pyroxene grains are common and dispersed throughout the matrix phyllosilicates.

Ungrouped C2 chondrite Essebi is similar in mineralogy to Bells, having abundant chondrules and fragments of olivine and pyroxene as well as phyllosilicate-rich matrix and magnetite. However, the abundance of anhydrous minerals (olivine and pyroxene) is higher compared to that of Bells and magnetite is less abundant. Fine-grained rims surrounding chondrules are frequently observed.

Tagish Lake is an ungrouped C2 carbonaceous chondrite and highly brecciated containing chondrules, mineral fragments, rare altered CAIs, abundant magnetite, complex carbonates and Fe,Ni-sulfides of various composition. All mineral phases are embedded into a fine-grained, phyllosilicate-rich matrix, which has a very high porosity compared to other carbonaceous chondrites (Brown et al., 2000; Zolensky et al., 2002). Chondrules, AOAs, and

CAIs are commonly surrounded by compact fine-grained rims similar to those in CM chondrites, Bells, and Essebi. Occasionally, larger clumps of compact matrix material can be observed (Fig. 1f). The sample of Tagish Lake used in this study is not one of those samples, which have been collected immediately after fall and kept frozen, and thus potentially has been in contact with liquid water on Earth.

4. Hydrogen isotopic composition of phyllosilicate-rich matrix

Here we report on δD values obtained from various clasts in three HEDs (NWA 7542, EET 87513 and Saricicek), three polymict ureilites (Dar al Gani 319, Dar al Gani 999, and EET 83309), two CR chondrites (Al Rais and Renazzo), and one H chondrite (Sahara 98645), as well as from different lithologies in the CI chondrite Ivuna and the ungrouped C2 chondrites Bells, Essebi, and Tagish Lake for comparison (Table 3, Figs. 3, 4, 5). Potential major hosts of hydrogen are organic matter and phyllosilicates. The carbonaceous chondrites Al Rais, Renazzo, Ivuna, Bells, Essebi, and Tagish Lake are known to contain various amounts and types of organic matter embedded on different scales within the phyllosilicate-rich matrix (Alexander et al., 2007, 2010; Le Guillou et al., 2014). It is therefore not possible to obtain the D/H ratio of pure phases. The influence of organic matter on analyses will be discussed in section 5.1. The reported mean C/H and Si/H ratios can be compared to those reported in the literature for bulk carbonaceous chondrites (for C/H see, e.g., Alexander et al., 2012). We note that the C/H ratios given in Alexander et al (2012) are for wt%, i.e., should be divided by a factor of 12 when compared to our results which are given as atomic ratios. Mean values of C/H ratios determined here fall well within the range determined by Alexander et al. (2012) for bulk carbonaceous chondrites when the estimated uncertainty of a factor 2 due to matrix effects on the SIMS C^-/H^- sensitivity factor is considered (see section 2). It was found here that Si/H and C/H ratios vary considerably within and between individual ion images from different clasts. For example, the integrated Si/H and C/H ratios of individual images from the studied clasts vary from 0.1 to 4.6 (Si/H) and from 0.01 to 1.0 (C/H), respectively (Table 3). In Fig. 5 (and additionally in Fig. S1), D/H vs. Si/H and C/H ratios are shown for selected samples; to construct these figures individual ion images were subdivided into 1.25 x 1.25 µm²-sized areas and areas with similar Si/H and C/H ratios combined to represent a single data point ("binning", bin sizes are 0.2 for Si/H and 0.04 for C/H). The size of 1.25 µm is only somewhat larger than the size of D-rich hotspots (0.6 - 1 µm; Fig. 6) and permits to obtain sufficiently precise H isotope data for individual bins. For the samples Al Rais, EET 83309, DaG 999, NWA 7542, Essebi, and Bells we observe moderate to good correlations in D/H vs. Si/H over the whole range of observed Si/H ratios

(Figs. 5 and S1). On the other hand, good correlations in D/H vs. C/H, were observed only for analyses on Ivuna, Tagish Lake, Renazzo, and DaG 999 over the whole range of C/H ratios (Fig. 5).

In addition, we observed large variations in D/H within individual ion images. Examples of three D-hotspots in Bells, Al Rais, and in a CM-like clast from Saricicek are shown in Fig. 6.

In five cases (Renazzo, Ivuna, Essebi, Bells, Tagish Lake) we can compare our D/H data of matrix material with bulk data from the literature (see below). Except for Renazzo, we find a satisfactory agreement between our data and those from the literature. This is remarkable given the fact that our studies are based on measurements of only limited amounts of material, but the findings show that our measurements can be considered representative when compared to bulk material.

4.1. CM-like clasts

For CM-like clasts, there is a clear systematic difference in the δD between fine-grained rims /matrix and TCI areas. On average, the δD-signature of TCI clumps (low Si/H) is lower compared to those of matrix-dominated areas (Table 3, Fig. 3). As expected, the Si/H ratio of matrix-dominated areas is higher compared to the TCI clumps or mixes of those.

The δD of CM-like clast NWA 7542-10 ranges from -60 to 300 ‰ (Fig. 3; Table 3). CM-like clasts Saricicek-01 and Saricicek-02 show a δD variation from -220 to +340 ‰, which is larger than the variation observed for the CM-like clast in NWA 7542 (Fig. 3; Table 3). Two clasts (-01 and -02) from the howardite EET 87513 have δD values from -10 to +340 ‰, as similarly observed for NWA 7542. A 1 µm-sized D hotspot associated with C-rich matter having a δD of 6200 ± 500 ‰ was observed in clast 01 of Saricicek (Fig. 6).

The average of all analyses on CM-like clasts is +100 ± 30 ‰. Average C/H and Si/H ratios are 0.08 ± 0.01 and 0.96 ± 0.14, respectively.

4.2. CI-like clasts from HEDs, ordinary chondrites, and ureilites

CI-like clasts NWA 7542-1, NWA 7542-6, and NWA 7542-7 (HED) are indistinguishable from each other in their hydrogen isotopic composition having δD values from +200 to +640 ‰ (Fig. 4; Table 3). D/H ratios are positively correlated with Si/H ratios, but not with C/H ratios. Averages of all analyses on CI-like clasts in NWA 7542 are +270 ± 50 ‰ for δD, 0.65 ± 0.08 for C/H, and 2.88 ± 0.25 for Si/H.

The CI-like clast from the H chondrite Sahara 98645 has δD values from -290 to +270 ‰ with an average of +100 ± 160 ‰. Neither the Si/H ratio nor the C/H ratio correlate with the D/H ratio of matrix areas of the clast. The analyses yielded an average C/H ratio of 0.12 ± 0.02 and a Si/H ratio of 1.60 ± 0.217.

CI-like clasts Nos. 3, 5, and 10 from the polymict ureilite DaG 319 are texturally CI-like and similar to the CI-like clasts in NWA 7542 (see chapter mineralogy and Patzek et al., 2018a; Table 2). δD values range from +950 to +3100 ‰. The average δD is 2040 ± 290 ‰. Neither the Si/H nor the C/H ratio is correlated with D/H (Fig. 5). Average C/H and Si/H ratios are 0.22 ± 0.04 and 1.57 ± 0.11, respectively. The δD-values of the four CI-like clasts Nos. 5, 6, 9, and 10 from the polymict ureilite EET 83309 range from +1650 to +2400 ‰ with an average value of +1870 ± 80 ‰ (Fig. 4; Table 3). The variation of D/H in clasts from EET 83309 is less extreme compared to that of clasts from DaG 319 but shows a similar high enrichment in D. The Si/H ratio as well as the C/H ratio is well correlated with the D/H ratio (Fig. 5). Only one area each in two clasts in the polymict ureilite DaG 999 were analyzed. Their average δD is +1220 ‰ (Fig 4). Positive correlations are observed for D/H vs. Si/H and D/H vs. C/H (Fig. 5).

The overall averages of CI-like clasts in ureilites are δD = +1900 ± 110 ‰, C/H = 0.35 ± 0.04, and Si/H = 2.08 ± 0.13.

4.3. CI-like clasts from CR chondrites

D/H was measured in five CI-like clasts from the CR chondrites Al Rais and Renazzo and in the interstitial matrix of Renazzo. δD values of three CI-like clasts in Al Rais range from +740 to +1520 ‰ (Fig. 4; Table 3). A 600 nm-sized D hotspot associated with C-rich matter having a δD of 24000 ± 3000 ‰ was observed in clast 1 of Al Rais (Fig. 6). Two CI-like clasts from Renazzo have δD values from +1730 to + 2480 ‰. The two clasts from Renazzo have on average a much higher δD when compared to that from Al Rais (2060 ‰ vs. 1060 ‰). δD values in matrix from Renazzo range from +1400 to +1850 ‰ with an average of 1590 ‰. This is clearly higher than the δD value of +703 ‰ reported for a bulk sample of Renazzo (Alexander et al., 2012). The CI-like clast Al Rais 01 (4x2.5 mm^2) is the largest in this thin section and has slightly variable δD values (+740 to +1240 ‰).

For clasts from Al Rais we observed a positive correlation between D/H and Si/H but not between D/H and C/H, whereas the opposite is true for the CI-like clasts and matrix from Renazzo (Fig. 5). The D excesses of CI-like clasts in CR chondrites are generally of similar magnitude as those of CI-like clasts in polymict ureilites and clearly higher compared to CI-like clasts in HEDs or CI chondrites in general (Fig. 4). The overall averages of CI-like clasts in CR chondrites are δD = +1540 ± 150 ‰, C/H = 0.44 ± 0.05, and Si/H = 2.93 ± 0.18.

4.4. Ivuna, Bells, Essebi, and Tagish Lake

Within the brecciated CI chondrite Ivuna (Morlok et al., 2004), the δD-values of different analyzed areas vary from -170 to +950 ‰, with an average of 210 ± 190 ‰ (Table 3, Fig. 4).

Within error, this agrees with the δD value of +80 ‰ determined for a bulk sample of Ivuna (Alexander et al., 2012). The D/H ratio mainly correlates with the C/H ratio but less clear with the Si/H ratio (Fig. 5). Average C/H and Si/H ratios are 0.41 ± 0.13 and 1.43 ± 0.60, respectively.

The δD values of selected areas in Bells range from +270 to +540 ‰ with an average of 380 ± 50 ‰ (Table 3; Fig. 4). Within the 2σ error, this agrees with the δD value of +317 ‰ determined for two bulk samples of Bells (Alexander et al., 2012). Average C/H and Si/H ratios are 0.83 ± 0.06 and 1.70 ± 0.14, respectively. The D/H ratio correlates with the Si/H but not with the C/H ratio. A 1 µm-sized D hotspot associated with a slight enrichment in C having a δD of 16800 ± 1600 ‰ was observed in one of the analyzed areas in Bells (Fig. 6). Essebi is similarly enriched in D, with δD values ranging from +230 to +900 ‰ and an average of +360 ± 120 ‰. Within error, this agrees with the δD value of +338 ‰ determined for a bulk sample of Essebi (Alexander et al., 2012). The D/H ratio correlates with the Si/H but not with the C/H ratio. Average C/H and Si/H ratios are 0.53 ± 0.05 and 1.30 ± 1.73, respectively. δD values of Tagish Lake obtained in this study vary from +30 to +1410 ‰ with an average of +120 ± 210 ‰ taking all spots into account (Table 3; Figs. 4, 6). Average C/H and Si/H ratios are 0.63 ± 0.07 and 0.63 ± 0.76, respectively. Within 2σ error, this agrees with the δD value of +535 ‰ determined for three bulk sample of Tagish Lake (Alexander et al., 2012). The D/H ratio correlates with the C/H but not with the Si/H ratio. However, spots 1 and 2 analyzed on Tagish Lake revealed clearly lower enrichments in D relative to the other four spots (δD = 100 and 30 ‰, respectively, vs. δD = 650 to 1400 ‰). These two spots also yield H count rates one order of magnitude higher compared to those of the other four. Their Si/H ratio is also significantly lower (Table 3).

5. Discussion

The δD signatures and mineralogical aspects of the different clasts can be used as fingerprints to investigate possible relationships between the clasts and already known carbonaceous chondrite groups. Different processes, which will be discussed here, are able to modify the δD signature of clasts: Since organic matter in carbonaceous chondrites is known to be enriched in D, we will comment on the influence of organic matter, although organic molecules and aggregates are not the main topic of this work. Weathering of the meteoritic samples is also a process able to modify δD signatures. Additionally, a possibly heterogeneous distribution of D in the phyllosilicates and organic matter has to be taken into account for the interpretation of the data.

Recently, Piani et al. (2018) developed an analytical protocol to analyze the hydrogen isotope composition of the water component in phyllosilicates with SIMS by utilizing a Cs primary ion beam. By using D^-/H^- and the C^-/H^- ratio and by extrapolating the D/H at C/H=0 the authors obtain the D/H ratio of the water component in C-free phyllosilicates. This has been applied to CM (Piani et al., 2018) and CV chondrites (Piani and Marrocchi, 2018). It is not the primary goal of the work presented here to determine individual H components in CI- and CM-like clasts but to see how they differ in D/H from bulk CI and CM chondrites. Only for the CM clasts we will infer the D/H of water as it can be directly compared to the results obtained with SIMS by Piani et al. (2018) for CM chondrites.

5.1. Influence of organic matter on the δD data

Organic matter can occur either as insoluble or as soluble components in carbonaceous chondrites. While the latter cannot be separately analyzed, the insoluble component (IOM) can be isolated from the bulk meteorite by acid demineralization. Soluble organic matter (SOM) is hard to recognize in thin sections, since it might have been lost during sample preparation involving solvents. Organic matter in aqueously-altered carbonaceous chondrites is enriched in deuterium compared to the phyllosilicate fraction of these meteorites (Alexander et al., 2010, 2012 and references therein). During aqueous alteration, it is likely that organic matter and its D signature is redistributed into the phyllosilicates (Le Guillou et al., 2014) through ion exchange. The spatial distribution of the organic matter generally depends on the meteorite and, more specifically, on the degree of alteration and the size of the phyllosilicates (Le Guillou et al., 2014). For example, the δD signatures of various lithologies in the CI chondrite Ivuna overlap with those of bulk determinations. Additionally, the degree of aqueous alteration (abundance of anhydrous silicates) of Ivuna and CI-like clasts in HEDs and polymict ureilites is very similar (cf. Patzek et al., 2018a) and they have been altered at similar temperatures (Visser et al., 2018).

The C/H ratio can help to constrain the amount of organic matter within analyzed areas. Since IOM in primitive carbonaceous chondrites is usually enriched in D and represents a significant fraction of carbon, a positive correlation between δD and the C/H ratio has been observed for whole-rock samples of some meteorites (Alexander et al., 2010, 2012; Piani et al. 2015). For some of the samples analyzed here, especially the CI-like clasts and primitive carbonaceous chondrites, we observe a correlation between δD and the C/H ratio (Fig. 5). Exceptions from this are CI-like clasts from DaG 319, NWA 7542, and Al Rais, and the C2 chondrites Essebi and Bells. In our work, we identified clearly visible D hotspots, ≤1 µm in size, in Bells (~17000 ‰), Al Rais (~24000 ‰), and the CM-like clast Saricicek-1

(~6000 ‰). However, organic material with SMOW-like δD does also occur in close proximity to the observed hotspots in Bells and Al Rais. This illustrates that D/H does not necessarily have to be well correlated with C/H at the scales considered here. However, we cannot rule out the possibility of tiny epoxy blobs appearing as SMOW-like C-rich grains in ion images, but based on D/H vs. C/H ratios we can rule out substantial contamination by epoxy during analyses (see also section 2).

5.2. Effects of weathering

Terrestrial weathering is an important process when discussing highly volatile elements such as hydrogen, oxygen, or nitrogen, since these elements can easily be exchanged when in contact with the terrestrial environment. Meteorites analyzed in this study have been recovered from hot deserts (DaG 319, DaG 999, NWA 7542, Sahara 98645), somewhat warm climates (Al Rais, Ivuna, and Bells), and cold deserts (EET 83309). The howardite Saricicek is a fresh fall, and fragments were collected starting from the day after the fall. The CR chondrite Renazzo is also a fall. However, Renazzo fell in 1824 and the conditions under which the sample has been stored cannot be reconstructed. Based on D/H, Si/H, and C/H ratios of the fresh fall Saricicek and cold desert Antarctic find EET 83309 and those from hot desert finds (e.g. NWA 7542, DaG 319, and DaG 999), no clear indication for distinct alteration features such as excess H due to formation of hydroxides (and therefore a more SMOW-like D/H ratio) can be found in those from hot deserts (see paragraph 4.2 and 4.4 and Figs. 3,4). For the CI-like clasts in ureilites, there is less variation for the D/H data obtained on EET 83309 compared to those from DaG 319 and DaG 999. Previous investigations on bulk samples propose that samples from Antarctica are less altered than those from hot deserts (cf. supplement of Alexander et al., 2012). This finding could potentially be interpreted as a more intense alteration in DaG 319 and DaG 999 compared to EET 83309. However, this does not have any influence on the discussion of these results.

The CR chondrite Al Rais is affected by terrestrial weathering, evidenced by replacement of metal grains by Fe-hydroxides. Polymict ureilites DaG 319 and EET 83309 also show terrestrial alteration. For EET 83309, H exchange was apparently not as intense as it was for hot desert finds such as DaG 319 or NWA 7542 (Alexander et al., 2012).

Besides macroscopic effects such as replacement of Fe-metal, terrestrial alteration also affects the organic matter in the matrix of carbonaceous chondrites in general. Alexander et al. (2007) showed that the IOM contents of the paired Algerian CR chondrites (El Djouf 001 and Acfer 059, 186, and 209; Bischoff et al., 1993a) are an order of magnitude lower than in less-weathered meteorites, and their elemental and isotopic compositions of the IOM also differ from those of the less-weathered ones (δD = 2600–3000‰ and H/C = 0.75-0.81 vs. δD = 120–428 ‰ and H/C = 0.4-0.53).

Generally, terrestrial weathering is able to change the δD signature of meteoritic samples. Some samples can be more susceptible to terrestrial weathering than others depending on their porosity. For example, Tagish Lake has very high porosity compared to the polymict ureilites DaG 319 or EET 83309 (Brown et al., 2000; Zolensky et al., 2002), which could result in much easier infiltration by terrestrial fluids. For the Tagish Lake sample used in this study, we cannot exclude a (partial) interaction with terrestrial fluids as described in section 3.4. However, taking special care in selecting samples and areas within the sample can help to reduce the risk of analyzing areas affected by terrestrial weathering, such as cracks filled with FeOH-phases.

5.3. Heterogeneity within single clasts

The distribution of individual minerals within CM- and CI-like clasts is heterogeneous. Some analyzed clasts exhibit a large range in δD values, e.g., clast DaG 319-03, in which the averaged δD values of individual 20 x 20 μm^2-sized areas range from +1700 to +3100 ‰ (Table 3). As already explained in chapter 5.1, the influence of organic matter on the obtained δD values has to be considered, since the organic matter is potentially enriched in D relative to mineral phases. Interestingly, we observe a positive correlation between δD and Si/H ratio for many of the samples (Fig. 5). This positive correlation either indicates that the water/OH^- bound in phyllosilicates (high Si/H) is enriched in D, or that very little but extremely D-rich organics are finely-intergrown with phyllosilicates below the resolution of the NanoSIMS. The latter requires, however, that the amount of the extremely D-rich organics is very low since we do not always observe a positive correlation in C/H vs. D/H. D-enriched water has been observed previously by various groups (e.g. Deloule and Robert, 1995; Grossman et al., 2000; Bonal et al. 2013). Being able to resolve this correlation in D/H vs. Si/H for most CI-like clasts in ureilites and those from CR chondrites, suggests the presence of abundant D-rich phyllosilicates (i.e., water) within this type of clasts, even though our approach is not optimized for these complex mixtures.

Since the hydrogen-bearing phyllosilicates are products of secondary alteration on the parent body, their alteration itself could lead to fractionation of H and D on a local scale by the possible escape of hydrogen from its formation environment. Depending on the abundance of different precursor phases, the alteration can differ and, therefore, produce different D/H ratios on various scales within a single clast, increasing the D/H variability on a sub-mm scale. Large fractionation between H and D are possible when large fractions of the oxidizing component (i.e., water) are consumed. However, unlike primitive ordinary chondrites such as

Semarkona (e.g. Alexander et al., 2012), CI-like clasts still contain high amounts of hydrogen, which makes it doubtful that hydrogen in CI-like clasts experienced a large isotope fractionation.

5.4. CM-like clasts share features with brecciated CM chondrites

Based on mineralogy, mineral chemistry as well as the hydrogen isotopic composition, the CM-like clasts can clearly be linked to CM2 chondrites in general (see also; Zolensky et al., 1996; Gounelle et al., 2003, 2005; Mittlefehldt, 2015; Patzek et al., 2018a). Common TCI (tochilinite-cronstedtite-intergrowth) clumps, chondrules, and the phyllosilicate-rich matrix are typical components in CM2 chondrites and occur in varying abundances and within fragments of various degree of alteration in different CM2 chondrites such as Cold Bokkeveld or Nogoya (e.g., Metzler et al., 1992; Lindgren et al., 2013; Bischoff et al., 2017; Lentfort et al., 2019). This variability can also be observed within the population of volatile-rich clasts, which have been investigated within this work. Some clasts show a well-preserved chondritic texture with well-defined chondrules surrounded by accretionary dust rims and large clasts of TCI embedded into a fine-grained matrix material similar to the rims. Other clasts are dominated by a clastic fine-grained matrix lacking chondrules and/or accretionary dust rims surrounding the latter (Figs. 1a,b; see more details in Patzek et al., 2018a). Within the population of CM-like clasts, we therefore observe different lithologies of CM2 chondrites, which all may originate from different parent bodies or from an impacting CM2-breccia showing all of the described lithologies (e.g., Metzler et al., 1992; Buchanan et al., 1993; Lindgren et al., 2013; Bischoff et al., 2017; Zolensky et al., 2017; Lentfort et al., 2019). Such a breccia may then disintegrate in its primary lithologies during impact. Nevertheless, different lithologies in one CM-like clast can be observed as well (cf. Patzek et al., 2018a; e.g. EET 87513-01). As a side note shown in the results, the hydrogen isotopic composition of different components of the CM-like clasts, such as fine-grained matrix, accretionary dust rims, and TCI clumps, varies slightly (Fig. 3). Analyses of areas rich in TCI clumps are generally less enriched in D. This might be attributed to the process of aqueous alteration on the respective parent body and is accompanied by changes in other isotope systems, the mineralogy, and the structure of organic matter (Van Kooten et al., 2018). However, the data still overlap with literature data of bulk CM chondrites as well as with tochilinite-rich micrometeorites analyzed by Gounelle et al. (2005) (ranging in δD from -240 to +10 ‰; Fig. 7). Oxygen isotope analyses of similar clasts have been carried out in various studies and also support a link to CM chondrites (Buchanan et al., 1993; van Drongelen et al., 2016, Patzek et al., 2018b).

Taking all features of these clasts into account, the CM-like clasts seem to be clearly related to CM2 chondrites. High textural and mineralogical variability reflects the brecciation of most CM2 chondrites (e.g. Metzler et al., 1992; Zolensky et al., 1997, 2017; Rubin et al., 2007; Bischoff et al., 2006, 2017; Lentfort et al., 2019).

From a correlation between D^-/H^- and C^-/H^- Piani et al. (2018) inferred the D/H ratio of water in several CM chondrites by extrapolating D^-/H^- to $C^-/H^- = 0$. In principle we could do the same with the data for CM clasts. However, it should be noted that observed C/H ratios in our work extend to higher values than those of Piani et al. (2018) because of the much smaller spatial scale of our analyses and data reduction procedure. If we focus only on those C/H ratios in the range reported by Piani et al. (2018), i.e., $^{13}C^-/H^- < \sim 0.02$ which corresponds to C/H < ~0.3 in our work, then for CM clasts in EET 87513 and NWA 7542 there are good correlations between D/H and C/H (Fig. S1; a linear regression gives χ^2 values of 1.02 and 1.07, respectively). By extrapolating to C/H = 0 we obtain δD = +59 ± 45 ‰ for EET 87513 and δD = -69 ± 27 ‰ for NWA 7542. These values are higher than what was inferred by Piani et al. (2018) for the water component in most CM chondrites (δD ~ -340 ‰) but are fully compatible with what was inferred for the least altered part of the CM chondrite Paris (δD = -69 ± 163 ‰), although CM-like clasts studied here are not of petrologic type 2.8 but rather 2.4 - 2.6.

5.5. CI-like clasts from different breccias originate from different parent bodies

Since the mineralogy and thermal history of CI-like clasts from different host rocks is very similar (cf. Patzek et al., 2018a; Visser et al., 2018), the isotopic data of CI-like clasts from each host rock can therefore be compared to each other and to carbonaceous chondrites. This led to the observation of significant differences between the different materials.

Comparing the CI-like clasts from HEDs with CI chondrites in general, one has to consider the brecciated character and the different lithologies of CI chondrites. All CI chondrites are regolith breccias consisting of lithologies having different mineralogy and "bulk" chemistry (Endress et al., 1994; Morlok et al., 2006). A direct comparison to a "typical" CI chondrite may therefore not be feasible. Nevertheless, the δD of Ivuna varies from -170 to +950 ‰ (average of ~200 ‰), which overlaps with the range of the CI-like clasts from HEDs and ordinary chondrites but is clearly distinct from that of CI-like clasts from ureilites (Figs. 4,8; see next paragraph). The hydrogen isotopic composition of the CI-like clasts in HEDs (δD from +200 to +640 ‰) overlaps with data obtained for slightly different subtypes (magnetite-rich, olivine-rich/-poor microxenoliths) by Gounelle et al. (2005) also obtained in HEDs (δD from -280 to +300 ‰). This suggests that CI-like clasts from HEDs and those from ordinary chondrites are related to CI chondrites. The highly brecciated nature of CI chondrites may further explain the mineralogical variation of CI-like clasts in HEDs.

Despite the textural and mineralogical similarities between CI-like clasts from HEDs and those from polymict ureilites and CR chondrites, the hydrogen isotopic compositions of CI-like clasts from HEDs differ significantly (Figs. 4,8) compared to those from polymict ureilites and CR chondrites. The CI-like clasts from ureilites show a much wider range in their hydrogen isotopic composition, ranging from the upper value of CI chondrites to values exceeding those of CR chondrites (Fig. 4). In general, the overall δD signatures of CI-like clasts in polymict ureilites are clearly different from those in Ivuna (Fig. 8), while C/H and Si/H ratios are similar. This implies again that the overall element abundances in the phyllosilicate-rich matrix are similar, however the isotopic composition differs.

When comparing CI-like clasts from different meteorite groups with mineralogical data from Bells, none of the CI-like clasts from the investigated meteorites match the typical characteristics of Bells (e.g. abundant chondrules and anhydrous silicate fragments, although Bells is also rich in magnetite). Taking the δD signatures and the mineralogical features into account, it is unlikely that they originate from the same parent body (Fig. 9).

The δD values of selected CI-like areas in Essebi yield similar values to Essebi's bulk value of +340 ‰ (Fig. 9; Alexander et al., 2012). Comparing Essebi with CI-like clasts from ureilites, Essebi has more chondrules and anhydrous mineral fragments compared to CI-like clasts in ureilites (Figs. 1 and 2; Table 2). Thus, based on the mineralogy and δD signatures, we cannot establish a link between CI-like clasts from ureilites and Essebi .

Literature data of bulk samples (Engrand et al., 2003; Alexander et al., 2012) are compatible with the average δD value of Tagish Lake from this work when ignoring spots 1 and 2 (Fig. 9). Since the count rates of these two spots were one order of magnitude higher and their δD signature is clearly different from the other spots measured on Tagish Lake, these spots might be contaminated by terrestrial weathering. This is also in agreement with textural evidence for diffusive Fe-enrichment and cross-cutting Fe-enriched veins, which can be observed in the SEM. Thus, based on mineralogical aspects, the high matrix porosity, and the maximum δD value of 1400 ‰, we cannot establish a link between Tagish Lake and CI-like clasts from ureilites (Fig. 1; Table 2), although Tagish Lake does contain areas similarly enriched in magnetite grains.

The obtained δD-signatures of CI-like clasts in the CR chondrite Al Rais are lower compared to those from Renazzo (+740 to +1520 ‰ vs. +1730 to 2480 ‰; Table 3; Figs. 4, 9). These values overlap quite well with the data for CI-like clasts in polymict ureilites ranging from +950 to ~+3100 ‰ (Table 3; Figs. 4,8). In general, bulk CR chondrites are enriched in D, and IOM can be highly-enriched up to >2500 ‰ (Guan and Zolensky, 1997; Alexander et al., 2007, 2012; Bonal et al. 2013). δD-signatures obtained from matrix material of Renazzo (i.e., not CI-like clasts) yield enrichments of ~1590 ‰ on average, indicating a slightly lower enrichment in D when compared to CI-like clasts in Renazzo itself (Fig. 8). The D/H ratios of matrix material are clearly higher than the bulk D/H data from the literature (δD = 703 ‰; Alexander et al., 2012). There are several explanations to account for this discrepancy: (i) All matrix measurements reported here were made in close proximity (~100 µm) of a CI-like clast, and it cannot be excluded that isotope equilibration between H from the clast and from the surrounding matrix material accounts for this. (ii) It is possible that (true) large-scale D/H heterogeneities exist in Renazzo. These possible heterogeneities have been reported earlier by Bonal et al. (2013) (iii) If Renazzo samples would have been inappropriately stored for almost 200 years, D/H ratios might have been affected in different samples differently. However, this explanation is rather speculative since storage conditions of these historical samples are generally good.

The chondrules found within the clasts in polymict ureilites are significantly smaller than the average chondrule size in CR chondrites (Weisberg et al., 1993). CI-like clasts in CR chondrites occasionally contain "microchondrules" with sizes of ~100 µm, which are very similar in size to the two observed chondrules (~100 µm and ~150 µm) and well below the common chondrule sizes in CR chondrites (Weisberg and Prinz, 1991; Bischoff et al., 1993a; Weisberg et al., 1993; Endress et al., 1994). Taking the similar mineralogy (especially the occasional occurrence of microchondrules), chemical compositions, and the δD values of the CI-like clasts in CR chondrites and in polymict ureilites into account, they might share a common origin (Table 2; Fig. 8). In case of the CR chondrites, the CI-like clasts had to be incorporated into the final parent body after the last episode of aqueous alteration on the first generation CR chondrite parent body, since the clasts show clear borders to chondrule rims and "normal" CR matrix (Endress et al., 1994) and the bulk rocks are unbrecciated on the thin section scale. Thus, the aqueous alteration, which led to the alteration of the CI-like parent body (the precursor rocks of the CI-like clasts), could not have happened after the accretion of the CR chondrites as discussed in detail by Patzek et al. (2018a). Taking the formation age of the CR chondrite parent body into account (>4 Ma after CAI; Schrader et al., 2017), and since the alteration of the clasts must have happened before incorporation, these clasts were formed and altered very early in the Solar System. Mn-Cr dating of carbonates within these clasts may help to constrain the episode(s) of alteration, but requires further surveys to identify a sufficient amount with sizes allowing in-situ dating.

5.6. Evidence for D-rich ices?

As previously discussed, the H in aqueously-altered chondrites can be bound as a OH component in phyllosilicates formed during the reaction of the anhydrous silicates with water and in organic matter (either in SOM or IOM). Following, the δD signature is a mixture of different components, which can have different D/H ratios. As shown in Fig. 5, positive, statistically significant correlations between δD and Si/H ratios can be seen for CI-like clasts from polymict ureilites EET 83309 and DaG 999 and the CR chondrite Al Rais. Linear regressions of D/H vs. Si/H in CI-like clasts yield D/H = $(4.69 \pm 0.41) \times 10^{-5} \times$ Si/H + $(3.34 \pm 0.10) \times 10^{-4}$ (χ^2=2.11, included in errors) for EET 83309, $(7.03 \pm 1.14) \times 10^{-5} \times$ Si/H + $(2.04 \pm 0.23) \times 10^{-4}$ (χ^2=1.80, included in errors) for DaG 999, and $(2.45 \pm 0.09) \times 10^{-5} \times$ Si/H + $(2.59 \pm 0.09) \times 10^{-4}$ (χ^2=1.54, included in errors) for Al Rais. Additionally, the CI-like clasts from ureilites DaG 999, and CR chondrite Renazzo show a positive correlation between δD and the C/H ratio (Fig. 5), as observed for whole-rock data of some primitive carbonaceous chondrites and in the in situ studies by SIMS of CM chondrites (Piani et al., 2018) and CV chondrites (Piani and Marrocchi, 2018). Linear regressions yield D/H = $(9.83 \pm 1.95) \times 10^{-4} \times$ C/H + $(2.64 \pm 0.19) \times 10^{-4}$ for DaG 999 (χ^2=0.40) and $(3.47 \pm 0.42) \times 10^{-4} \times$ C/H + $(3.41 \pm 0.17) \times 10^{-4}$ (χ^2=1.45, included in errors) for Renazzo. All zero intercepts indicate D/H ratios higher than SMOW in CI-like clasts with δD values between 300 and 1200 ‰. The correlations suggest the presence of a Si-rich, H-poor, and C-poor component with high D/H (e.g., δD ~3000 ‰ as similarly observed for D-rich phyllosilicates in CR and ordinary chondrites; Deloule and Robert, 1995), a C-rich component with high D/H (organics), and a Si-poor and C-poor component with comparatively low D/H. Since phyllosilicates (Si-rich) in the CI-like clasts are a dominant phase and the δD-signature correlates positively with the Si/H ratio, it seems reasonable to attribute this to an apparent enrichment of D within the phyllosilicates. D-rich OH bound in phyllosilicates together with D-rich organics may explain the overall enrichment in D compared to the other type of clasts. These D-rich signatures bound in the phyllosilicates could either be the result of a homogenization during aqueous alteration with the D-rich organics or a primary signature resulting from the incorporation of D-rich ices into the parent body(ies) of the CI-like clasts in ureilites. A similar scenario might be true for the CI-like clasts in CR chondrites, although we only observe a positive correlation of δD with Si/H for the clasts in Al Rais.

Whether D-rich water in phyllosilicates is a proxy for the signature of the original water modifying this material is unclear because exchange reactions or diffusive loss can never be ruled out, although the peak temperature for the CI- and CM-like clasts has been determined to be 65±25 °C, arguing against any quantitative loss of H from phyllosilicates

(Visser et al. 2018). Robert and Deloule (1995) clearly pointed out that phyllosilicates in Renazzo and Semarkona are carriers of D-rich water. Likely production mechanisms for D-rich water are ion-molecule reactions in cold and dense regions of the Solar System's molecular cloud core or protoplanetary disk. These pristine D-rich ices may have later reacted with anhydrous silicates in the solar nebula to form D-rich phyllosilicates present in the CI-like clasts in ureilites. In contrast, the water incorporated into the parent body(ies) of the CI-like clasts in the ordinary chondrite Sahara 98645, of those in the HED NWA 7542, and of CM-like clasts could have been formed at heliocentric distances similar to those of CI chondrites within the solar nebula. It has also been shown by Piani et al. (2018) that the CM chondrite Paris has been altered by water enriched in D relative to other CM chondrites. Based on this finding they propose a dual origin of water in carbonaceous chondrites in general and specifically in CM chondrites (Piani et al., 2018). This finding together with our results clearly favor a larger diversity of ice and water present in the early Solar System.

5.7. Different primitive material in inner and outer Solar System breccias

The existence of the CI-like clasts in several meteorite groups proves the existence of additional primitive material in the (early) Solar System besides the CI, CM, and CR chondrites. The CI-like clasts in CR chondrites and polymict ureilites experienced similar alteration histories, but they probably formed in different regions than other chondrites, e.g., the CI chondrites. The higher D enrichment of CI-like clasts in ureilites relative to CI chondrites might indicate that these clasts formed at even larger distance from the Sun and incorporated D-rich ices and organic material. Since the position of the snow line and the D/H ratio of the solar system evolved over time (e.g. Yang et al., 2013), it is not possible to determine the exact origin of these ices. Thus, the difference in D/H ratios might only reflect a spatial difference rather than a temporal one. The distribution of this material into achondrites is potentially the result of the disk instability introduced by the growth and movement of Jupiter.

Since the CI-like clasts in ureilites and CR chondrites have a different δD signature when compared to CI chondrites, these clasts are better referred to as C1 clasts, which indicates only their petrologic type and shows they have no genetic relation to CI1 (Ivuna-type) chondrites. This characterization is also supported by preliminary O isotope data (e.g. Patzek et al., 2019). How much of this early-formed material was available for the formation of the terrestrial planets or a late accretion onto them remains unknown, but it might have played an important role. Additionally, there are more samples from the early solar system available, e.g. interplanetary dust particles (IDPs) and Antarctic micrometeorites (AMMs).

However, these samples are generally of smaller sizes when compared to the clasts we are able to study in brecciated meteorites.

Aleon et al. (2001) reported on some IDPs, which exhibit δD signatures on the order of 800 and 5000 ‰. These IDPs have a fluffy carbonaceous nature, but they do not have a typical CI-like mineralogy. Engrand and Maurette (1998) published a survey on the mineralogy of ~800 AMMs. A subset was analyzed also for D/H ratios, which are largely incompatible with those of CR chondrites or with CI-like clasts in ureilites. In general, investigations aiming on the nature of IDPs and AMMs (e.g. Prasad et al., 2018) propose that there is a large variety of material formed in the early Solar System, which might be available today only as clasts. This is in good agreement with our conclusions.

6. Conclusions

We obtained D/H ratios of several CI and CM-like clasts from several different meteorites. In addition, we report on D/H data of several carbonaceous chondrites. Interestingly, for Ivuna, Essebi, Bells, and Tagish Lake inferred average δD-signatures based on total integrated counts are only slightly higher than bulk data when available (e.g. Alexander et al., 2012), indicating that we are able to obtain comparable results on these complex carbonaceous chondrites using our approach, although it has been proposed that the emission of H from organics is usually favored when using Cs^+ ions.

Based on the mineralogy and δD signatures, three distinct groups of carbonaceous chondrite-like material have been identified as clasts:

(1) CI-like clasts in HEDs and ordinary chondrites, which have a similar δD signature compared to CI chondrites and are also of petrologic type 1.

(2) CI-like clasts in polymict ureilites and CR chondrites, which both have a similar mineralogy when compared to CI chondrites, but are more enriched in D. Thus, these types of clasts are better referred to as C1 clasts rather than CI-like.

(3) CM-like clasts in HEDs, which are unambiguously CM chondrite fragments based on δD signatures, mineralogy, and O-isotopes (Buchanan et al., 1993; van Drongelen et al., 2016).

Since C1 clasts from ureilites and those from CR chondrites are indistinguishable in their δD signature and mineralogy, they seem to share a common origin. This type of clast is not represented as individual bulk meteorite samples in today's sample collections and can therefore bear important information about processes taking place in the early Solar System. Since CR chondrites are generally unbrecciated and the C1 clasts in them have sharp borders with surrounding material, the C1 clasts must have been available at the time of accretion of the final parent body. This makes it necessary for the aqueous alteration on the parent body of the C1 clasts to have ended before the C1 clasts were incorporated into the CR chondrite parent body during accretion. Nonetheless, material from the C1 parent body had to have been distributed into the orbit of the ureilite parent body(ies) after its planetary differentiation; this material was then incorporated into the regolith of the ureilite parent body(ies). Whether this ureilite parent body was the first generation parent body or a re-accreted rubble pile asteroid after the catastrophic disruption cannot be answered based on the available data; however, from asteroid 2008 TC3 (Almahata Sitta) we know that different generations of ureilite parent bodies existed (Bischoff et al., 2010; Goodrich et al., 2014, 2017, 2018; Horstmann and Bischoff, 2014). The existence of the C1 clasts in several meteorite groups proves the existence of additional primitive, volatile-rich material in the (early) Solar System besides the CI, CM, and CR chondrites, but maybe also apart from micrometeorites, which display a wide compositional and textural variety. The C1 clasts experienced a similar alteration history as the CI chondrites but probably formed in a different region.

Acknowledgements

U. Heitmann is thanked for skillful preparation work. We further thank T. Grund for keeping the SEM running, E. Gröner and Philipp Schuhmann for maintaining the NanoSIMS, E. Hauri and L. Nittler for H isotope standards, and C. Brennecka for editorial support. We also thank the Associated Editor Eric Quirico, Larry Nittler, and two anonymous reviewers for their fruitful comments and suggestions. We acknowledge the Division of Meteorites of the Smithsonian, the Meteorite Working Group at the Johnson Space Center, the Natural History Museum of Vienna, the University of Parma, and Mike Zolensky for contributing samples. This work was supported by the German Research Foundation (DFG) within the SFB-TRR 170 “Late Accretion onto Terrestrial Planets” (subproject B5). This is TRR 170 publication No. 80.

References

Aléon, J., Engrand, C., Robert, F. and Chaussidon, M. (2001) Clues to the origin of interplanetary dust particles from the isotopic study of their hydrogen-bearing phases. *Geochimica et Cosmochimica Acta* **65(23)**, 4399-4412.

Alexander C. M. O'D., Fogel M., Yabuta H. and Cody G. (2007) The origin and evolution of chondrites recorded in the elemental and isotopic compositions of their macromolecular organic matter. *Geochimica et Cosmochimica Acta* **71**, 4380-4403.

Alexander C. M. O'D., Newsome S., Fogel M., Nittler L., Busemann H. and Cody G. (2010) Deuterium enrichments in chondritic macromolecular material—Implications for the origin and evolution of organics, water and asteroids. *Geochimica et Cosmochimica Acta* **74**, 4417-4437.

Alexander C. M. O'D., Bowden R., Fogel M. L., Howard K. T., Herd C. D. and Nittler L. R. (2012) The provenances of asteroids, and their contributions to the volatile inventories of the terrestrial planets. *Science* **337**, 721-723.

Alexander, C. M. O'D., Cody, G. D., De Gregorio, B. T., Nittler, L. R., and Stroud, R. M. (2017) The nature, origin and modification of insoluble organic matter in chondrites, the major source of Earth's C and N. *Chemie der Erde-Geochemistry*, **77(2)**, 227-256.

Bischoff A., Palme H., Spettel B., Clayton R.N. and Mayeda T. K. (1988) The chemical composition of dark inclusions from the Allende meteorite. *Lunar and Planetary Science* XIX, 88 - 89, Lunar and Planetary Institute, Houston.

Bischoff, A., Palme, H., Ash, R., Clayton, R., Schultz, L., Herpers, U., Stöffler, D., Grady, M., Pillinger, C. and Spettel, B. (1993a) Paired Renazzo-type (CR) carbonaceous chondrites from the Sahara. *Geochimica et Cosmochimica Acta* **57**, 1587-1603.

Bischoff A., Palme H., Schultz L., Weber D., Weber H.W., and Spettel B. (1993b) Acfer 182 and paired samples, an iron-rich carbonaceous chondrite: Similarities with ALH 85085 and relationship to CR chondrites. *Geochimica et Cosmochimica Acta* **57**, 2631-2648.

Bischoff A., Scott E. R. D., Metzler K. and Goodrich C. A. (2006) Nature and origins of meteoritic breccias. In *Meteorites and the Early Solar System II*, edited by Lauretta D.S. and. McSween Jr H.Y. Tucson.:Univ. of Arizona. pp. 679-712.

Bischoff A., Horstmann M., Pack A., Laubenstein M. and Haberer S. (2010) Asteroid 2008 TC_3 - Almahata Sitta: A spectacular breccia containing many different ureilitic and chondritic lithologies. *Meteoritics & Planetary Science* **45**, 1638–1656.

Bischoff A., Ebert S., Metzler K. and Lentfort S. (2017) Breccia classification of CM chondrites (#6089). *Meteoritics & Planetary Science* **52**, A26.

Bischoff A., Schleiting M., Wieler R., and Patzek M. (2018) Brecciation among 2280 ordinary chondrites – constraints on the evolution of their parent bodies. *Geochimica et Cosmochimica Acta* **238**, 516-541.

Brearley A. J. and Jones R. H. (1998) Chondritic meteorites. *Planetary Materials*, edited by Papike J.J. Washington: Mineralogical Society of America. pp 3-1 – 3-398.

Brearley A. J. and Prinz M. (1992) CI chondrite-like clasts in the Nilpena polymict ureilite. Implications for aqueous alteration processes in CI chondrites. *Geochimica et Cosmochimica Acta* **56**, 1373-1386.

Bonal, L., Alexander, C. O., Huss, G., Nagashima, K., Quirico, E. and Beck, P. (2013) Hydrogen isotopic composition of the water in CR chondrites. *Geochimica et Cosmochimica Acta* **106**, 111-133.

Briani, G., Gounelle, M., Bourot-Denise, M. and Zolensky, M. E. (2012) Xenoliths and microxenoliths in H chondrites: Sampling the zodiacal cloud in the asteroid Main Belt. *Meteoritics & Planetary Science* **47**, 880-902.

Brown P. G., Hildebrand A. R., Zolensky M. E., Grady, M., Clayton R. N., Mayeda T. K., Tagliaferri E., Spalding R., MacRae N. D., Hoffman E. L., Mittlefehldt D. W., Wacker J. F., Bird J. A., Campbell M. D., Carpenter R., Gingerich H., Glatiotis M., Greiner E., Mazur M. J., McCausland P. J., Plotkin H. and Rubak Mazur T. (2000) The fall, recovery, orbit, and composition of the Tagish Lake meteorite: a new type of carbonaceous chondrite. *Science* **290**, 320-325.

Buchanan P. C., Zolensky M. E. and Reid A. M. (1993) Carbonaceous chondrite clasts in the howardites Bholghati and EET87513. *Meteoritics & Planetary Science* **28**, 659-669.

Deloule, E., and Robert, F. (1995) Interstellar water in meteorites?. *Geochimica et Cosmochimica Acta*, 59(22), 4695-4706.

Endress M. and Bischoff A. (1996) Carbonates in CI chondrites: Clues to parent body evolution. *Geochimica et Cosmochimica Acta* **60**, 489-507.

Endress M., Keil K., Bischoff A., Spettel B., Clayton R.N. and Mayeda T.K. (1994) Origin of dark clasts in the Acfer 059/El Djouf 001 CR2 chondrite. *Meteoritics* **29**, 26-40.

Engrand, C. and Maurette, M. (1998) Carbonaceous micrometeorites from Antarctica. *Meteoritics & Planetary Science*, **33**(4), 565-580.

Engrand, C., Gounelle, M., Zolensky, M. E. and Duprat, J. (2003) About Tagish Lake as a Potential Parent Body for Polar Micrometeorites; Clues from Their Hydrogen Isotopic Compositions. *Lunar and Planetary Science Conference* (Vol. 34).

Funk C., Bischoff A. and Schlüter J. (2011) Xenoliths in carbonaceous and ordinary chondrites. *Meteoritics & Planetary Science* **46**, A71.

Goodrich C. A. and Keil K. (2002) Feldspathic and other unusual clasts in polymict ureilite DaG 165. *Lunar and Planetary Science Conference* **33**, #1777.

Goodrich C. A., Scott, E. R. D. and Fioretti A. M. (2004) Ureilitic breccias: Clues to the petrologic structure and impact disruption of the ureilite parent asteroid. *Chemie der Erde* **84**, 283-327.

Goodrich C. A., Bischoff A. and O'Brien D. P. (2014) Asteroid 2008 TC_3 and the fall of Almahata Sitta, a unique meteorite breccia. *Elements* **10,** 31-37.

Goodrich C.A., Fioretti A.M., Zolensky M., Fries M, Shaddad M., Kohl I., Young E. and Jenniskens P. (2017) A breccia of ureilitic and C2 carbonaceous chondrite materials from Almahata Sitta: Implications for the regolith of ureilitic asteroids. *Meteoritics & Planetary Science* 52, Special Issue: A107, #6214.

Goodrich C. A., Fioretti A. M., Zolensky M., Shaddad M., Ross D. K., Kohl I., Young E., Kita N., Hiroi T., Sliwinski M. G. and Jenniskens P. (2018) The Almahata Sitta Polymict Ureilite from the University of Khartoum Collection: Classification, Distribution of Clast Types in the Strewn Field, New Meteorite Types, and Implications for the Structure of Asteroid 2008 TC3. *Lunar and Planetary Science Conference* **49**, #1321.

Gounelle M., Zolensky M.E., Liou J.-C., Bland P.A. and Alard O. (2003) Mineralogy of carbonaceous chondritic microclasts in howardites: identification of C2 fossil micrometeorites. *Geochimica et Cosmochimica Acta* **67**, 507–527.

Gounelle M., Engrand C., Alard O., Bland P. A., Zolensky M. E., Russell S. S. and Duprat J. (2005) Hydrogen isotopic composition of water from fossil micrometeorites in howardites. *Geochimica et Cosmochimica Acta*, **69**, 3431-3443.

Greshake A. (2014) A strongly hydrated microclast in the Rumuruti chondrite NWA 6828: Implications for the distribution of hydrous material in the solar system. *Meteoritics & Planetary Science* **49**, 824–841.

Grossman J. N., Rubin A. E. and MacPherson G. J. (1988) ALH85085: A unique volatile-poor carbonaceous chondrite with possible implications for nebular fractionation processes. *Earth and Planetary Science Letters* **91**, 33-54.

Grossman, J. N., Alexander, C. M. O'D., Wang, J. and Brearley, A. J. (2000) Bleached chondrules: Evidence for widespread aqueous processes on the parent asteroids of ordinary chondrites. *Meteoritics & Planetary Science*, **35(3)**, 467-486.

Guan, Y. and Zolensky, M. E. (1997) The D/H ratios of round phyllosilicate and glass spherules in the Al Rais (CR) chondrite. Lunar and Planetary Science Conference **28**, 485.

Hoppe P., Cohen S. and Meibom A. (2013) NanoSIMS: Technical aspects and applications in cosmochemistry and biological geochemistry. *Geostandards Geoanalytical Res*. **37**, 111-154.

Horstmann M. and Bischoff A. (2014) The Almahata Sitta polymict breccia and the late accretion of Asteroid 2008 TC$_3$ - Invited Review. *Chemie der Erde - Geochemistry* **74**, 149-184.

Ikeda Y., Kita N. T., Morishita Y. and Weisberg M. K. (2003) Primitive clasts in the Dar al Gani 319 polymict ureilite: Precursors of the ureilites. *Antarctic Meteorite Research* **16**, 105-127.

Johnson C. A. and Prinz M. (1993) Carbonate compositions in CM and CI chondrites and implications for aqueous alteration. *Geochimica et Cosmochimica Acta* **57**, 2843-2852.

Lentfort, S., Bischoff, A., Ebert, S., (2019) Classification of 13 CM chondrite breccias and CM clasts in two achondrites (abstract #6029). *Meteoritics & Planetary Science* **54** #6029.

Lindgren P., Lee M.R., Sofe M. R. and Zolensky M. E. (2013) Clasts in the CM2 carbonaceous chondrite Lonewolf Nunataks 94101: Evidence for aqueous alteration prior to complex mixing. *Meteoritics & Planetary Science* **48**, 1074–1090.

Le Guillou C., Bernard S.,Brearley A. J. and Remusat L. (2014) Evolution of organic matter in Orgueil, Murchison and Renazzo during parent body aqueous alteration: In situ investigations. *Geochimica et Cosmochimica Acta* **131**, 368-392.

Metzler K., Bischoff A. and Stöffler D. (1992) Accretionary dust mantles in CM chondrites: evidence for solar nebula processes. *Geochimica et Cosmochimica Acta*, **56**, 2873-2897

Morlok, A., Bischoff, A., Stephan, T., Floss, C., Zinner, E. and Jessberger, E. K. (2006) Brecciation and chemical heterogeneities of CI chondrites. *Geochimica et Cosmochimica Acta* **70**, 5371-5394.

Mittlefehldt D. W. (2015) Asteroid (4) Vesta: I. The howardite-eucrite-diogenite (HED) clan of meteorites. *Chemie der Erde-Geochemistry* **75**, 155-183.

Patzek M., Hoppe P., Bischoff A., Visser R. and John T. (2017) Water-Bearing, Volatile-Rich Clasts in Howardites and Polymict Ureilites Carriers of Deuterium-Enriched Waters Not Sampled by Individual Meteorites. *Meteoritics & Planetary Science* **52**, A267.

Patzek, M., Bischoff, A., Visser, R., and John, T. (2018a) Mineralogy of volatile-rich clasts in brecciated meteorites. *Meteoritics & Planetary Science* **53**, 2519-2540.

Patzek M., Pack A., Bischoff A., Visser R., and John T. (2018b) O-isotope composition of CI- and CM-like clasts in ureilites, HEDs, and CR chondrites. *Meteoritics & Planetary Science* **53** (abstract 6254).

Patzek, M., Bischoff, A., Hoppe, P., Pack, A., Visser, R., and John, T. (2019) Oxygen and Hydrogen Isotopic Evidence for the Existence of Several C1 Parent Bodies in the Early Solar System. *Lunar and Planetary Science Conference*, **50**, #1779.

Piani, L. and Marrocchi, Y. (2018) Hydrogen isotopic composition of water in CV-type carbonaceous chondrites. *Earth and Planetary Science Letters* **504**, 64–71.

Piani, L., Remusat, L. and Robert, F. (2012) Determination of the H isotopic composition of individual components in fine-scale mixtures of organic matter and phyllosilicates with the nanoscale secondary ion mass spectrometry. *Analytical chemistry*, **84(23)**, 10199-10206.

Piani L., Robert F. and Remusat L. (2015) Micron-scale D/H heterogeneity in chondrite matrices: A signature of the pristine solar system water?. *Earth and Planetary Science Letters* **415**, 154-164.

Piani, L., Yurimoto, H. and Remusat, L. (2018) A dual origin for water in carbonaceous asteroids revealed by CM chondrites. *Nature Astronomy* **2**, 317–323.

Prasad, M. S., Rudraswami, N. G., de Araujo, A. A. and Khedekar, V. D. (2018) Characterisation, Sources and Flux of Unmelted Micrometeorites on Earth During the Last~ 50,000 Years. *Scientific reports*, **8(1)**, 8887.

Prinz M., Weisberg M. K., Nehru C. E. and Delaney J. S. (1987) EET83309, a polymict ureilite: Recognition of a new group. *Lunar and Planetary Science Conference* **18**, 802-803.

Rubin A. E., Trigo-Rodríguez J. M., Huber H. and Wasson J. T. (2007) Progressive aqueous alteration of CM carbonaceous chondrites. *Geochimica et Cosmochimica Acta*, **71**, 2361-2382.

Schrader D. L., Nagashima K., Krot A. N., Ogliore R. C., Yin Q., Amelin Y., Stirling C. H. and Kaltenbach A. (2017) Distribution of 26 Al in the CR chondrite chondrule-forming region of the protoplanetary disk. *Geochimica et Cosmochimica Acta* **201**, 275-302.

Scott E. R. D. (1988) A New Kind of Primitive Chondrite, Allan-Hills-85085. *Earth and Planetary Science Letters* **91**, 1-18.

van Drongelen K. D., Rumble III D. and Tait K. T. (2016) Petrology and oxygen isotopic compositions of clasts in HED polymict breccia NWA 5232. *Meteoritics & Planetary Science* **51**, 1184-1200.

van Kooten, E.M.M.E., Cavalcante, L.L., Nagashima, K., Kasama, T., Balogh, Z.I., Peeters, Z., Hsiao, S.S.Y., Shang, H., Lee, D.C., Lee, T., Krot, A.N. and Bizzarro, M., 2018. Isotope record of mineralogical changes in a spectrum of aqueously altered CM chondrites. *Geochimica et Cosmochimica Acta* **237**, 79–102.

Visser, R., John, T., Menneken, M., Patzek, M., Bischoff, A., (2018) Temperature constraints by Raman spectroscopy of organic matter in volatile-rich clasts and carbonaceous chondrites. *Geochimica et Cosmochimica Acta* **241**, 38-55.

Visser, R., John, T., Patzek, M., Bischoff, A., and Whitehouse, M. J. (2019) Sulfur isotope study of sulfides in CI, CM, C2ung chondrites and volatile-rich clasts–Evidence for different generations and reservoirs of sulfide formation. *Geochimica et Cosmochimica Acta* **261**, 210-223.

Weisberg M. K. and Prinz M. (1991) El Djouf 89001 - a new CR2 chondrite. *Meteoritics* **26**, 406.

Weisberg M. K., Prinz M. and Nehru C. E. (1988) Petrology of ALH85085: A chondrite with unique characteristics. *Earth and Planetary Science Letters* **91**, 19-32.

Weisberg M. K., Prinz M., Clayton R. N. and Mayeda T. K. (1993) The CR (Renazzo-type) carbonaceous chondrite group and its implications. *Geochimica et Cosmochimica Acta* **57**, 1567-1586.

Yang, L., Ciesla, F. J., and Alexander, C. M. O'D. (2013) The D/H ratio of water in the solar nebula during its formation and evolution. *Icarus*, **226**, 256-267.

Zolensky M.E., Weisberg M.K., Buchanan P.C. and Mittlefehldt D.W. (1996) Mineralogy of carbonaceous chondrite clasts in HED achondrites and the moon. *Meteoritics & Planetary Science* **31**, 518-537.

Zolensky M. E., Mittlefehldt D. W., Lipschutz M. E., Wang M., Clayton R. N., Mayeda T. K., Grady, M. M., Pillinger C. and David B. (1997) CM chondrites exhibit the complete petrologic range from type 2 to 1. *Geochimica et Cosmochimica Acta* **61**, 5099-5115.

Zolensky M. E., Nakamura K., Gounelle M., Mikouchi T., Kasama T., Tachikawa O., and Tonui E. (2002) Mineralogy of Tagish Lake: An ungrouped type 2 carbonaceous chondrite. *Meteoritics & Planetary Science* **37**, 737-761.

Zolensky, M., Gregory, T., Takenouchi, A., Nishiizumi, K., Treiman, A., Berger, E., Le, L., Fagan, A., Velbel, M., Imae, N., Yamaguchi, A., (2015) CM carbonaceous chondrite lithologies and their space exposure ages. *NIPR Annual Conference on Antarctic Meteorites*, 226-227.

Zolensky M.E., M. Fries, J. Utas, Q.H.-S. Chan, Y. Kebukawa, A. Steele, R.J. Bodnar, M. Ito, D. Nakashima, T. Nakamura, R. Greenwood, Z. Rahman, L. Le and D.K. Ross. (2016)

C chondrite clasts in H chondrite regolith breccias: Something different (abstract). *Meteoritics & Planetary Science* **51**, #6488.

Zolensky M., Takenouchi A., Gregory T., Nishiizumi K., Caffee M., Velbel M., Ross K., Zolensky A., Le L. and Imae N. (2017) The Relationship Between Cosmic-Ray Exposure Ages And Mixing Of CM Chondrite Lithologies. *Lunar and Planetary Science Conference* **48**, #2094.

Tables

Table 1: List of samples and the analyzed clast types.

sample	group	analyzed clast types	analyzed area [µm^2]
NWA 7542	poly. Eucrite	CM- and CI-like	1200 and 3200
Saricicek	Howardite	CM-like	3200
EET 87513	Howardite	CM-like	4800
Dar al Gani 319	poly. Ureilite	CI-like	2800
Dar al Gani 999	poly. Ureilite	CI-like	800
EET 83309	poly. Ureilite	CI-like	4800
Sahara 98645	H chondrite	CI-like	1200
Al Rais	CR chondrite	CI-like	3200
Renazzo	CR chondrite	CI-like and “host matrix”	2000 and 1600
Ivuna	CI chondrite		2000
Bells	$C2_{ung}$		2000
Essebi	$C2_{ung}$		2000
Tagish Lake	$C2_{ung}$		2400

Table 2: Typical characteristics of CM- and CI-like clasts from various host meteorites. For more details of CI- and CM-like clasts, we refer to Patzek et al. (2018a).

Type	**CM-like**	**CI-like**	**CI-like**	**CI-like**	**CI-like**
Host	HED	HED	ureilites	CR	OC
Size	<100 µm to 5 mm	<100 µm to 0.5 mm	<100 µm to 5 mm	<100 µm to 6 mm	<100 µm to 0.5 mm
Magnetite	rare	common	common	common	common
Sulfides	pyrr, pent	pyrr, rare pent	pyrr, rare pent	pyrr, rare pent	pyrr, rare pent
Anhydrous silicates	common; chondrules and fragments	very rare; fragments	rare; fragments and chondrules	rare; fragments and chondrules	very rare; fragments
Carbonates	mostly calcite/aragonite	rare; variable mineralogy	rare; variable mineralogy	rare; variable mineralogy	rare-abundant; variable mineralogy
Remarks	common TCI, accretionary dust rims	rare phosphates	rare phosphates	rare phosphates	

Pyrr = pyrrhotite; pent = pentlandite; TCI=Tochilinite-Cronstedtite-Intergrowth

Table 3: δD values and D/H, C/H, and Si/H ratios of all analyzed areas sorted by meteorite groups and clast types. C/H and Si/H ratios are subject to systematic uncertainties due to possible matrix effects of at least a factor of 2.

Sample	Clast	D/H × 10^6 ± 1σ	δD [‰] ± 1σ	C/H	Si/H	Notes
polymict ureilites						
Dar al Gani 319 CI-like (3)						
DaG 319-10	CI-like	333 ± 35	1135 ± 224	0.11	1.41	
DaG 319-5	CI-like	304 ± 43	949 ± 276	0.10	2.04	
DaG 319-3	CI-like	644 ± 45	3132 ± 286	0.38	1.76	
DaG 319-3	CI-like	545 ± 57	2501 ± 363	0.27	1.34	
DaG 319-3	CI-like	450 ± 48	1888 ± 309	0.17	1.44	
DaG 319-3	CI-like	488 ± 77	2133 ± 495	0.19	1.15	
DaG 319-3	CI-like	420 ± 48	1699 ± 308	0.15	1.58	
	average	**474 ± 19**	**2042 ± 122**	**0.22**	**1.57**	
	sd		**287**	**0.04**	**0.11**	
Dar al Gani 999 CI-like (2)						
DaG 999-06	CI-like	369 ± 24	1366 ± 156	0.07	2.43	
DaG 999-02	CI-like	338 ± 17	1168 ± 110	0.10	1.63	
	average	**346 ± 16**	**1224 ± 103**	**0.08**	**1.86**	
EET 83309 CI-like (4)						
EET 83309-9	CI-like	500 ± 16	2207 ± 105	0.45	3.27	
EET 83309-9	CI-like	426 ± 11	1738 ± 70	0.56	2.16	
EET 83309-9	CI-like	510 ± 15	2276 ± 96	0.68	3.03	
EET 83309-9	CI-like	498 ± 23	2197 ± 148	0.23	2.23	
EET 83309-10	CI-like	491 ± 20	2151 ± 131	0.42	2.40	
EET 83309-10	CI-like	529 ± 22	2394 ± 138	0.64	2.26	
EET 83309-10	CI-like	524 ± 55	2361 ± 356	0.61	3.28	
EET 83309-6	CI-like	430 ± 12	1758 ± 76	0.39	2.33	
EET 83309-6	CI-like	413 ± 15	1650 ± 95	0.32	1.75	
EET 83309-6	CI-like	420 ± 12	1698 ± 79	0.60	2.02	
EET 83309-5	CI-like	438 ± 11	1812 ± 68	0.48	2.47	
EET 83309-5	CI-like	431 ± 10	1769 ± 61	0.48	1.72	
	average	**447 ± 8**	**1868 ± 49**	**0.50**	**2.24**	
	sd		**82**	**0.04**	**0.15**	
CI-like clasts in ureilites	**average**		**1904**	**0.35**	**2.08**	
	sd		**112**	**0.04**	**0.13**	
ordinary chondrite						
Sahara 98645 CI-like (1)						
Sah 98645-1	CI-like	160 ± 21	26 ± 132	0.09	1.28	

Sah 98645-1	CI-like	198	±	26	271	±	165	0.15	1.94	
Sah 98645-1	CI-like	111	±	41	-285	±	266	0.10	1.91	
	average	**171**	**±**	**15**	**98**	**±**	**98**	**0.12**	**1.60**	
	sd				**161**			**0.02**	**0.22**	
HED										
NWA 7542 CI-like (3)										
NWA 7542-1	CI-like	198	±	9	269	±	60	0.73	3.35	
NWA 7542-1	CI-like	217	±	11	396	±	68	0.78	3.50	
NWA 7542-1	CI-like	187	±	6	199	±	38	0.74	2.13	
NWA 7542-7	CI-like	255	±	21	639	±	134	0.49	4.59	
NWA 7542-7	CI-like	190	±	8	223	±	54	0.84	2.72	
NWA 7542-7	CI-like	191	±	10	227	±	61	0.59	3.11	
NWA 7542-6	CI-like	215	±	12	379	±	79	0.24	3.23	
NWA 7542-6	CI-like	202	±	11	297	±	70	0.33	3.45	
	average	**197**	**±**	**4**	**268**	**±**	**28**	**0.65**	**2.88**	
	sd				**51**			**0.08**	**0.25**	
Saricicek CM-like (2)										
Saricicek-1	CM-like	208	±	9	338	±	55	0.10	1.42	matrix
Saricicek-1	CM-like	198	±	8	269	±	50	0.09	0.93	matrix
Saricicek-1	CM-like	203	±	8	306	±	50	0.08	0.67	matrix
Saricicek-2	CM-like	205	±	8	319	±	53	0.16	1.06	matrix
Saricicek-1	CM-like	193	±	7	237	±	47	0.10	0.73	matrix/TCI
Saricicek-1	CM-like	181	±	7	160	±	44	0.04	0.73	matrix/TCI
Saricicek-1	CM-like	147	±	6	-56	±	37	0.02	0.40	TCI
Saricicek-2	CM-like	121	±	5	-223	±	32	0.04	0.16	TCI
	average	**180**	**±**	**3**	**155**	**±**	**22**	**0.07**	**0.71**	
	sd				**72**			**0.02**	**0.14**	
EET 87513 CM-like (2)										
EET 87513-02	CM-like	193	±	8	242	±	49	0.11	0.89	matrix
EET 87513-02	CM-like	209	±	8	340	±	53	0.16	1.07	matrix
EET 87513-02	CM-like	203	±	8	301	±	51	0.18	0.93	matrix
EET 87513-01	CM-like	191	±	8	229	±	51	0.10	1.21	matrix/TCI
EET 87513-01	CM-like	199	±	8	275	±	52	0.10	1.14	matrix/TCI
EET 87513-01	CM-like	181	±	7	161	±	46	0.05	0.95	matrix/TCI
EET 87513-02	CM-like	185	±	7	185	±	46	0.05	0.67	matrix/TCI
EET 87513-02	CM-like	186	±	7	194	±	48	0.06	0.99	matrix/TCI
EET 87513-02	CM-like	161	±	6	36	±	41	0.03	0.58	TCI
EET 87513-01	CM-like	158	±	6	15	±	40	0.01	0.48	TCI
EET 87513-02	CM-like	154	±	6	-12	±	38	0.01	0.37	TCI
EET 87513-02	CM-like	163	±	6	44	±	41	0.02	0.59	TCI
	average	**179**	**±**	**3**	**150**	**±**	**21**	**0.07**	**0.77**	
	sd				**35**			**0.02**	**0.08**	

NWA 7542 CM-like (1)										
NWA 7542-10	CM-like	202	±	9	299	±	60	0.24	3.54	matrix
NWA 7542-10	CM-like	160	±	4	25	±	29	0.04	1.48	TCI
NWA 7542-10	CM-like	147	±	4	-58	±	25	0.05	1.10	TCI
	average	**157**	**±**	**3**	**7**	**±**	**21**	**0.06**	**1.46**	
	sd				**108**			**0.07**	**0.76**	
CM-like clasts in HED	**average**				**104**			**0.07**	**0.96**	
	sd				**32**			**0.01**	**0.14**	
CR chondrites										
Al Rais CI-like (3)										
Al Rais-1	CI-like	338	±	8	1172	±	54	0.59	2.18	
Al Rais-1	CI-like	348	±	11	1237	±	73	0.50	3.55	
Al Rais-1	CI-like	270	±	6	737	±	41	0.62	1.86	
Al Rais-1	CI-like	299	±	10	920	±	67	0.86	2.48	
Al Rais-4	CI-like	350	±	10	1246	±	65	0.25	2.66	
Al Rais-4	CI-like	346	±	11	1221	±	72	0.32	3.08	
Al Rais-3	CI-like	364	±	15	1336	±	97	0.29	3.50	
Al Rais-3	CI-like	392	±	18	1517	±	113	0.26	3.71	
	average	**321**	**±**	**6**	**1062**	**±**	**37**	**0.52**	**2.51**	
	sd				**86**			**0.08**	**0.24**	
Renazzo CI-like (2)										
Renazzo-1	CI-like	434	±	22	1789	±	144	0.37	3.60	
Renazzo-1	CI-like	425	±	18	1729	±	113	0.32	2.52	
Renazzo-1	CI-like	494	±	20	2170	±	127	0.41	2.10	
Renazzo-2	CI-like	541	±	26	2476	±	167	0.52	3.53	
Renazzo-2	CI-like	534	±	24	2427	±	157	0.42	3.31	
	average	**477**	**±**	**10**	**2062**	**±**	**64**	**0.39**	**2.71**	
	sd				**156**			**0.03**	**0.30**	
CR chondrite all CI-like	**average**				**1537**			**0.44**	**2.93**	
	sd				**153**			**0.05**	**0.18**	
Renazzo Matrix										
Renazzo Matrix	Matrix	374	±	16	1402	±	102	0.19	2.33	
Renazzo Matrix	Matrix	433	±	17	1779	±	108	0.39	1.77	
Renazzo Matrix	Matrix	370	±	14	1373	±	92	0.26	1.65	
Renazzo Matrix	Matrix	443	±	18	1846	±	116	0.50	1.55	
	average	**403**	**±**	**8**	**1587**	**±**	**51**	**0.33**	**1.78**	
	sd				**124**			**0.07**	**0.17**	
CI chondrite Ivuna										

Ivuna		303	±	22	948	±	139	0.96	3.84
Ivuna		212	±	16	363	±	100	0.62	2.91
Ivuna		175	±	5	123	±	31	0.30	1.00
Ivuna		129	±	48	-169	±	309	0.79	4.56
Ivuna		232	±	15	489	±	95	0.99	2.89
	average	**188**	**±**	**5**	**207**	**±**	**30**	**0.41**	**1.43**
	sd				**187**			**0.13**	**0.60**
C2 chondrites									
Bells		239	±	7	535	±	42	0.83	1.53
Bells		235	±	11	509	±	69	0.85	2.16
Bells		210	±	6	351	±	39	0.93	1.86
Bells		197	±	6	266	±	37	0.96	1.36
Bells		208	±	6	333	±	37	0.64	1.90
	average	**215**	**±**	**4**	**380**	**±**	**26**	**0.83**	**1.70**
	sd				**52**			**0.06**	**0.14**
Essebi		263	±	17	687	±	110	0.29	4.25
Essebi		225	±	6	446	±	40	0.50	1.50
Essebi		192	±	4	231	±	28	0.57	0.77
Essebi		283	±	11	818	±	74	0.51	2.78
Essebi		297	±	26	904	±	167	0.53	4.49
	average	**212**	**±**	**4**	**362**	**±**	**27**	**0.53**	**1.30**
	sd				**124**			**0.05**	**0.73**
Tagish Lake (1)		172	±	4	103	±	23	0.68	0.40
Tagish Lake (2)		161	±	3	32	±	19	0.58	0.31
Tagish Lake (3)		296	±	16	899	±	100	0.75	2.83
Tagish Lake (4)		375	±	21	1406	±	136	0.44	4.49
Tagish Lake (5)		260	±	11	668	±	70	0.74	3.59
Tagish Lake (6)		272	±	11	746	±	72	0.96	4.23
	average (3-6)	**285**	**±**	**8**	**828**	**±**	**49**	**0.77**	**3.81**
	sd (3-6)				**166**			**0.11**	**0.37**
	average all	**174**	**±**	**3**	**120**	**±**	**19**	**0.63**	**0.63**
	sd all				**210**			**0.07**	**0.76**

Number of clasts analyzed is shown in parentheses; sd = standard deviation of mean; C/H and Si/H ratios are given in atom%.

Figure captions

Fig. 1: (a) CM-like clast (no. 11) within the polymict eucrite NWA 7542 contains chondrules or mineral fragments of Mg-rich olivine and pyroxene, which are surrounded by fine-grained rims. Additionally, Fe-rich lumps of tochilinite are spread throughout the clast. All components are embedded in a fine-grained matrix. (b) CM-like clast in the howardite Saricicek. TCIs, one CAI, carbonate grains and areas with clastic matrix can be found. (c) Area in Ivuna that is dominated by phyllosilicate matrix and magnetite grains. (d) Matrix from C2 chondrite Bells containing magnetite and olivine of different compositions. The matrix porosity is higher compared to that of Ivuna. (e) C2 chondrite Essebi is less enriched in magnetite grains than Bells and contains various fragments, which are enriched in Fe. Silicates are also more Fe-rich compared to those in Bells. (f) Matrix fragment (CI-like) in the Tagish Lake C2 chondrite sitting in a highly porous matrix consisting of phyllosilicates and anhydrous silicates such as olivine and pyroxene. Images are in BSE. Chd= chondrule; CAI= calcium aluminum-rich inclusion; TCI= tochilinite-cronstedtite intergrowth; Mag = magnetite; ol= olvine.

Fig. 2: (a) CI-like clast in the polymict eucrite NWA 7542, which is dominated by phyllosilicate matrix and magnetite grains. One Fa-rich olivine (ol) can be found in the center of the clast. (b) CI-like clast in the howardite Saricicek, containing magnetite grains embedded in an Fe-rich phyllosilicate matrix. (c) CI-like clast in the polymict ureilite DaG 319 with magnetite grains and framboids embedded within phyllosilicates. (d) CI-like clast in the polymict ureilite EET 83309 with a similar mineralogy. Additionally, it contains a now-filled pore space or pit with grains of lath-shaped pyrrhotite. (e) CI-like clasts from the polymict ureilite DaG 999. Common magnetite grains and a chondrule can be found. (f) CI-like clast in the CR chondrite Al Rais containing magnetite grains and lath-shaped pyrrhotite embedded within phyllosilicates. Images in BSE; ol= olivine; mag= magnetite; pyrr =pyrrhotite; phos= phosphate; chd= chondrule.

Fig 3: δD values of five CM-like clasts in the HED meteorites NWA 7542 (diamond), Saricicek (triangle), and EET 87513 (circles) range from -220 to +340 ‰. The weighted averages are shown by the larger symbols and errors are 1σ. Areas rich in TCI clumps are generally less enriched in D relative to more "matrix" dominated areas and are shown in light red (for Saricicek and EET 87513). The number of clasts is given in brackets.

Fig. 4: δD values of single analyses carried out on different clasts. The data are sorted by the host meteorite and their weighted averages are shown by the larger symbols. Analyses of matrix areas in CI-like clasts from polymict ureilites DaG 319, DaG 999, and EET 83309 range from +950 to +3100 ‰. CI-like clasts in the CR chondrites Al Rais and Renazzo have δD values from +740 to +2480 ‰. δD in a CI-like clast in the OC chondrite Sahara 98645 ranges from -290 to +270 ‰. C2 chondrites Bells, Essebi, and Tagish Lake have δD values from +260 to +540 ‰, +230 to +900 ‰, and +100 to +1400 ‰, respectively. Matrix areas in the CI chondrite Ivuna have δD values from -170 to +950 ‰. The number of clasts is given in brackets and errors are 1σ.

Fig. 5: D/H vs. Si/H and D/H vs. C/H ratios of 1.25 x 1.25 µm²-sized areas in CI-like clasts in ureilites (EET 83309, DaG 319, and DaG 999) and CR chondrites (Al Rais and Renazzo), and in the matrix of Renazzo and Ivuna. See text for details on data binning. For CI-like clasts in ureilites EET 83309 and DaG 999, there are positive correlations between D/H and Si/H , and for DaG 999 also for D/H vs. C/H. While D/H and Si/H ratios in CI-like clasts in Al Rais are positively correlated, this is not the case for CI-like clasts (and matrix) in Renazzo. In contrast, there are positive correlations between D/H and C/H in Renazzo, while this is not the case in Al Rais. For matrix in Ivuna, D/H and C/H are positively correlated but not D/H and Si/H. Si/H and C/H ratios of all samples span roughly the same ranges. C/H and Si/H ratios are subject to systematic uncertainties due to possible matrix effects (see section 2). Errors are 1σ.

Fig. 6: (a) The H and C ion images of this area in Bells are well correlated. A D-rich hotspot, with C/H = 1.4 and ~1 µm in size, can be seen in the D/H image (white circle); the δD value is 16800 ± 1600 ‰. The yellow circle encases a C-rich grain with normal D/H (120 ± 260 ‰, C/H = 1.1). (b) The H and C ion images of this area in Al Rais are well correlated. A D-rich hotspot, with C/H = 1.2 and ~600 nm in size, can be seen in the D/H image (white circle); the δD value is 24000 ± 3000 ‰. The yellow circle encases a C-rich grain with normal D/H (130 ± 300 ‰, C/H = 1.3). (c) A D-rich hotspot in a CM-like clast in Saricicek, with C/H = 0.35 and ~1 µm in size, can be seen in the D/H image (white circle); the δD value is 6200 ± 500 ‰. Scale bar in each image represents 5 µm.

Fig. 7: The δD signatures of areas in CM-like clasts obtained in this study and the range of literature data of similar clasts and bulk CM chondrites. The black bar represents bulk data for several CM chondrites (**, Alexander et al., 2012), and the grey bar gives the range of data obtained by Gounelle et al. (2005) for tochilinite-rich micrometeorites (***).Weighted averages of δD values of clasts obtained in this study (black open symbols) agree with literature data on bulk CM chondrites and data for tochilinite-rich micrometeorites obtained by Gounelle et al. (2005) within 2σ. The variation of individual data of single samples is large due to variation in the mineralogy.

Fig. 8: Ranges of δD values of individual measurement spots (colored bars) and weighted averages (symbols within colored bars) for samples from this study. δD-signatures of CI-like clasts obtained from the ureilites (DaG 319, DaG 999, and EET 83309, all yellow) are enriched in D by +950 to +3100 ‰. This range is similar to CI-like clasts in the CR chondrites Al Rais and Renazzo, which are enriched in D by +700 to +2500 ‰, respectively, and which show similar enrichments compared to CI-like clasts in ureilites. In addition, The CI-like clasts in CR chondrites are similarly enriched in D compared to the Renazzo matrix (black bar). Our range in δD for Renazzo matrix is higher compared to bulk data of CR chondrites obtained by Alexander et al. (2012, **). CI-like clasts in the polymict eucrite NWA 7542 and the H chondrite Sahara 98645 are only slightly enriched in D and overlap with data obtained for Ivuna and magnetite(Mt)-rich olivine-poor/-rich micro-xenoliths in HEDs (Gounelle et al., 2005, *). Data obtained for Ivuna are in good agreement with bulk

data for CI chondrites obtained by Alexander et al. (2012, **); CCM = carbonaceous chondrite microexenoliths.

Fig. 9: The δD signatures of areas in Bells, Essebi, Tagish Lake, and CI-like clasts from ureilites compared to literature data. Filled bars are data of this study. Weighted averages are given as symbols within the filled bars. Two weighted averages are given for Tagish Lake with the small triangle including highly H-rich (presumably terrestrial altered) regions and the large triangle excluding it. Single symbols are literature data from bulk samples obtained by Engrand et al. (2003) and Alexander et al. (2012). δD-data for Tagish Lake (b), Essebi (c), and Bells (d) from this study agree with those of bulk data within 2σ uncertainties. Even though CI-like clasts in ureilites and those from CR chondrites (a) partly overlap with Tagish Lake, their mineralogy and average δD values differ significantly. See discussion for details.

Fig. S1: D/H vs. Si/H and D/H vs. C/H ratios of 1.25 x 1.25 µm²-sized areas in Tagish Lake, for CI-like clasts in the polymict eucrite NWA 7542 and the H chondrite Sahara 98645 as well as data for CM-like clasts in NWA 7542, EET 87513 and Saricicek. C/H and Si/H ratios are subject to systematic uncertainties due to possible matrix effects (see section 2). Additionally, D/H vs. Si/H and D/H vs. C/H ratios for Bells and Essebi are shown. Errors are reported as 1σ.

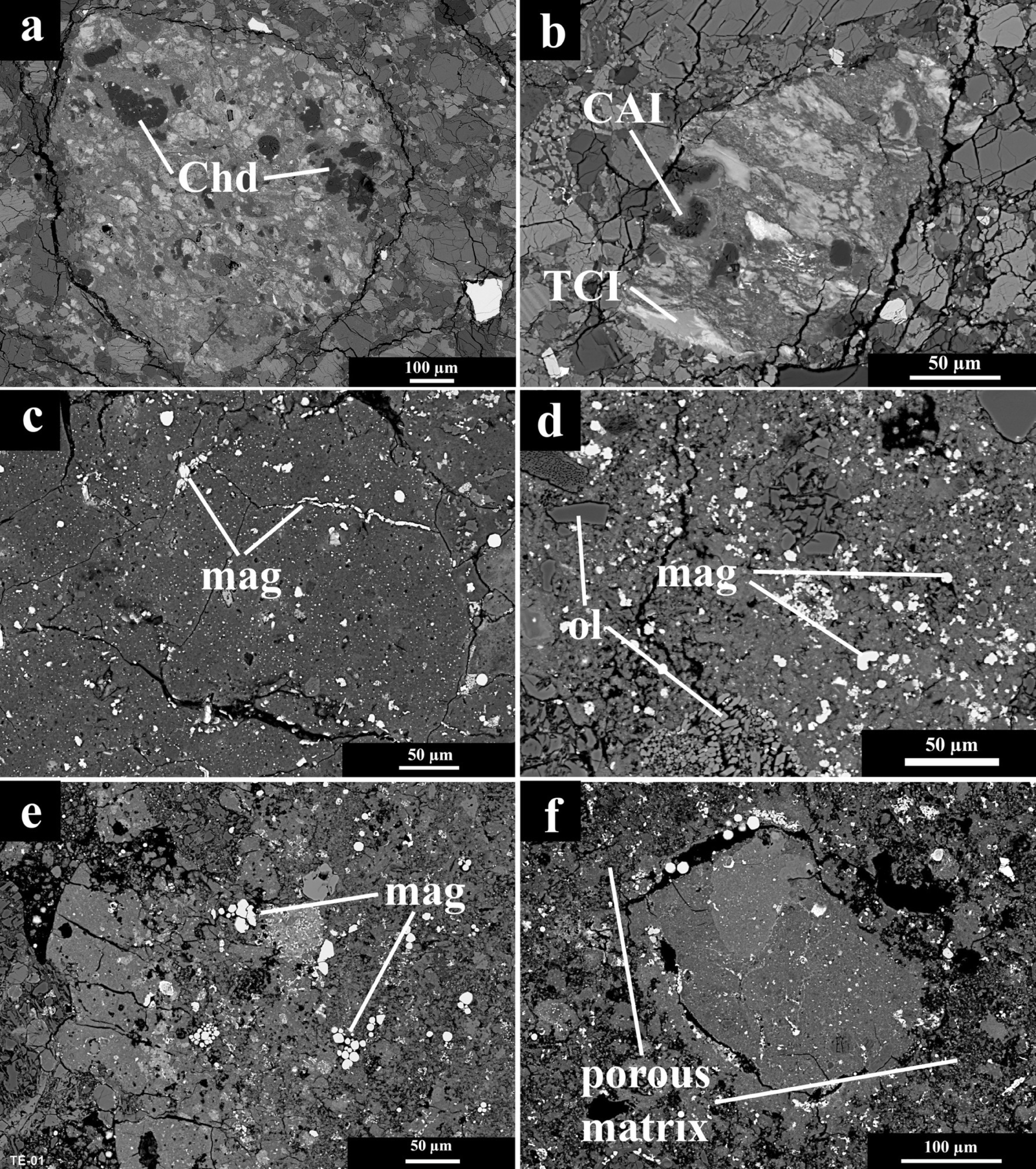

a
Chd
100 µm
b
CAI
TCI
50 µm
c
mag
50 µm
d
mag
ol
50 µm
e
mag
mag
50 µm
TE-01
f
porous
matrix
100 µm

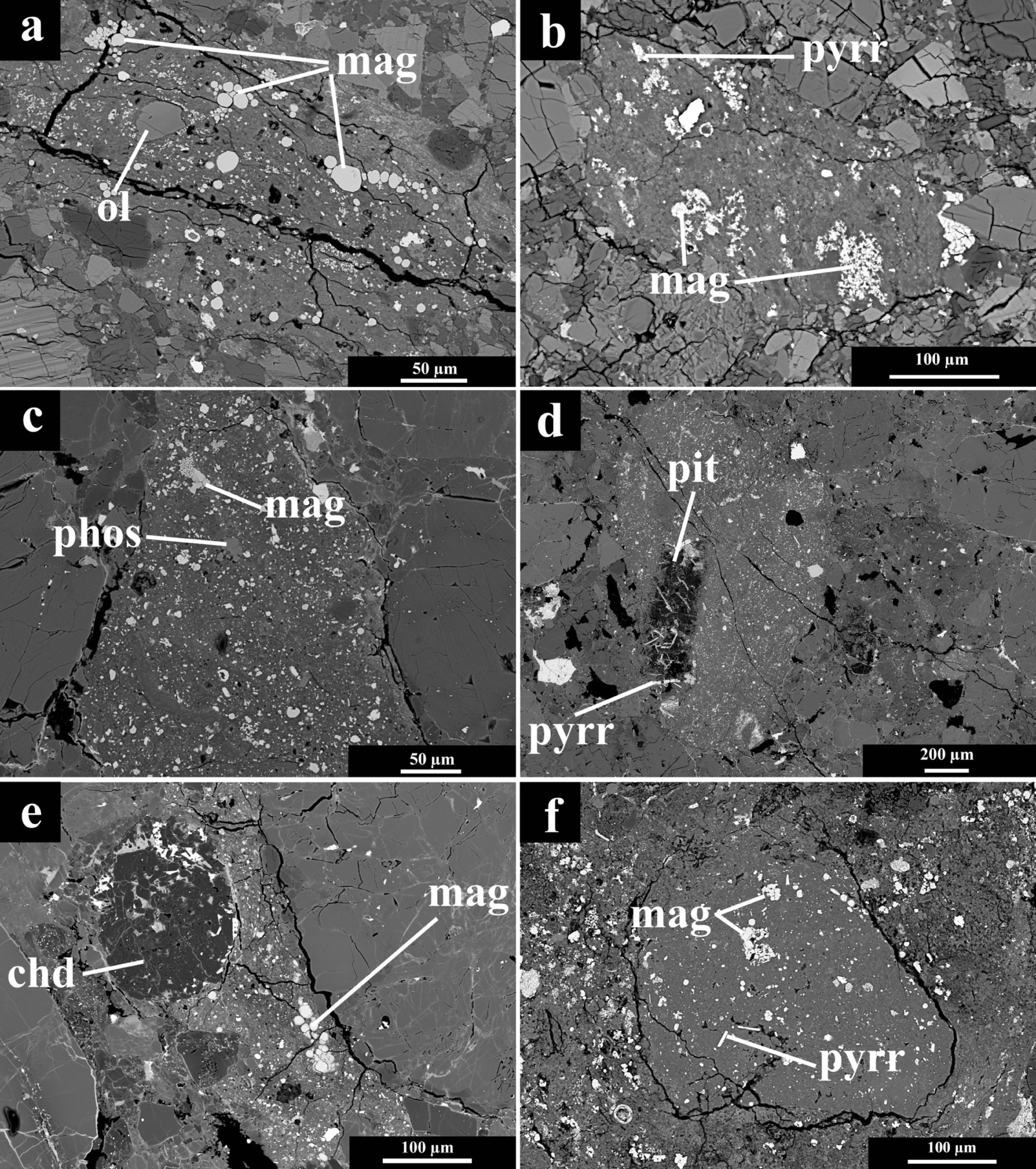
a
mag
ol
50 µm
b
pyrr
mag
100 µm
c
mag
phos
50 µm
d
pit
pyrr
200 µm
e
mag
chd
100 µm
f
mag
pyrr
100 µm

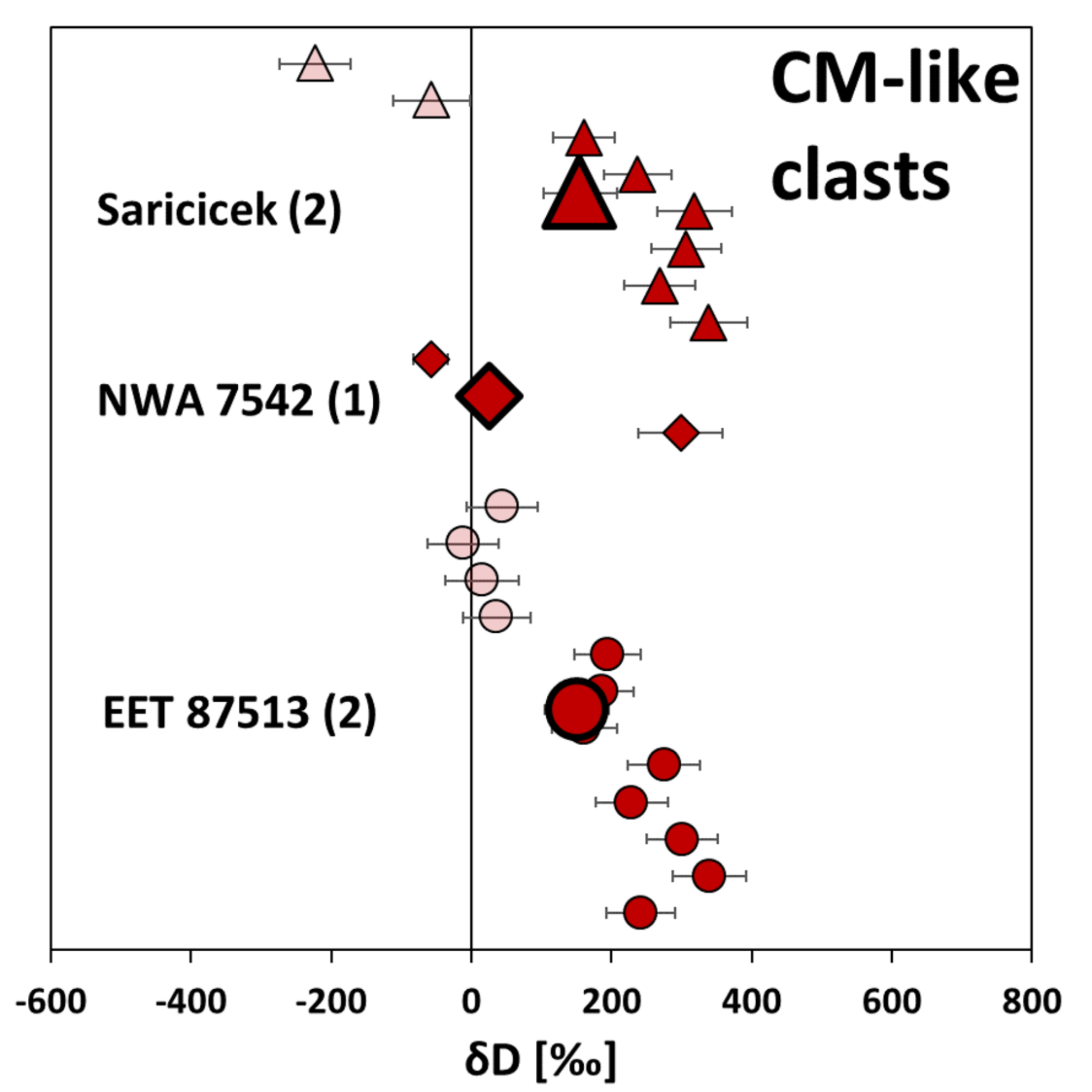

CM-like
clasts
Saricicek (2)
NWA 7542 (1)
EET 87513 (2)
-600
-400
-200
0
200
400
600
800
δD [‰]

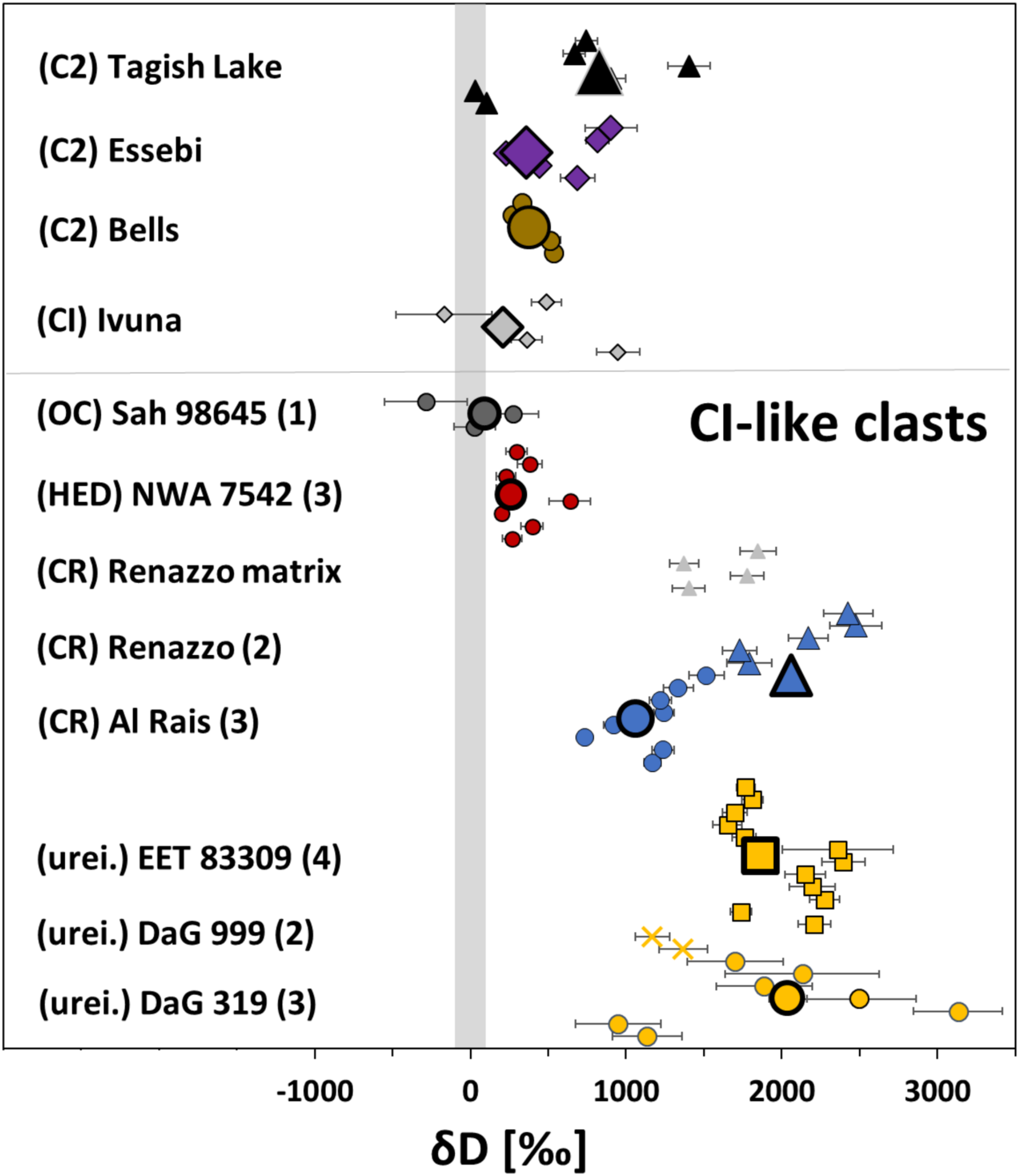
(C2) Tagish Lake
(C2) Essebi
(C2) Bells
(CI) Ivuna
(OC) Sah 98645 (1)
CI-like clasts
(HED) NWA 7542 (3)
(CR) Renazzo matrix
(CR) Renazzo (2)
(CR) Al Rais (3)
(urei.) EET 83309 (4)
(urei.) DaG 999 (2)
(urei.) DaG 319 (3)
-1000
0
1000
2000
3000
δD [‰]

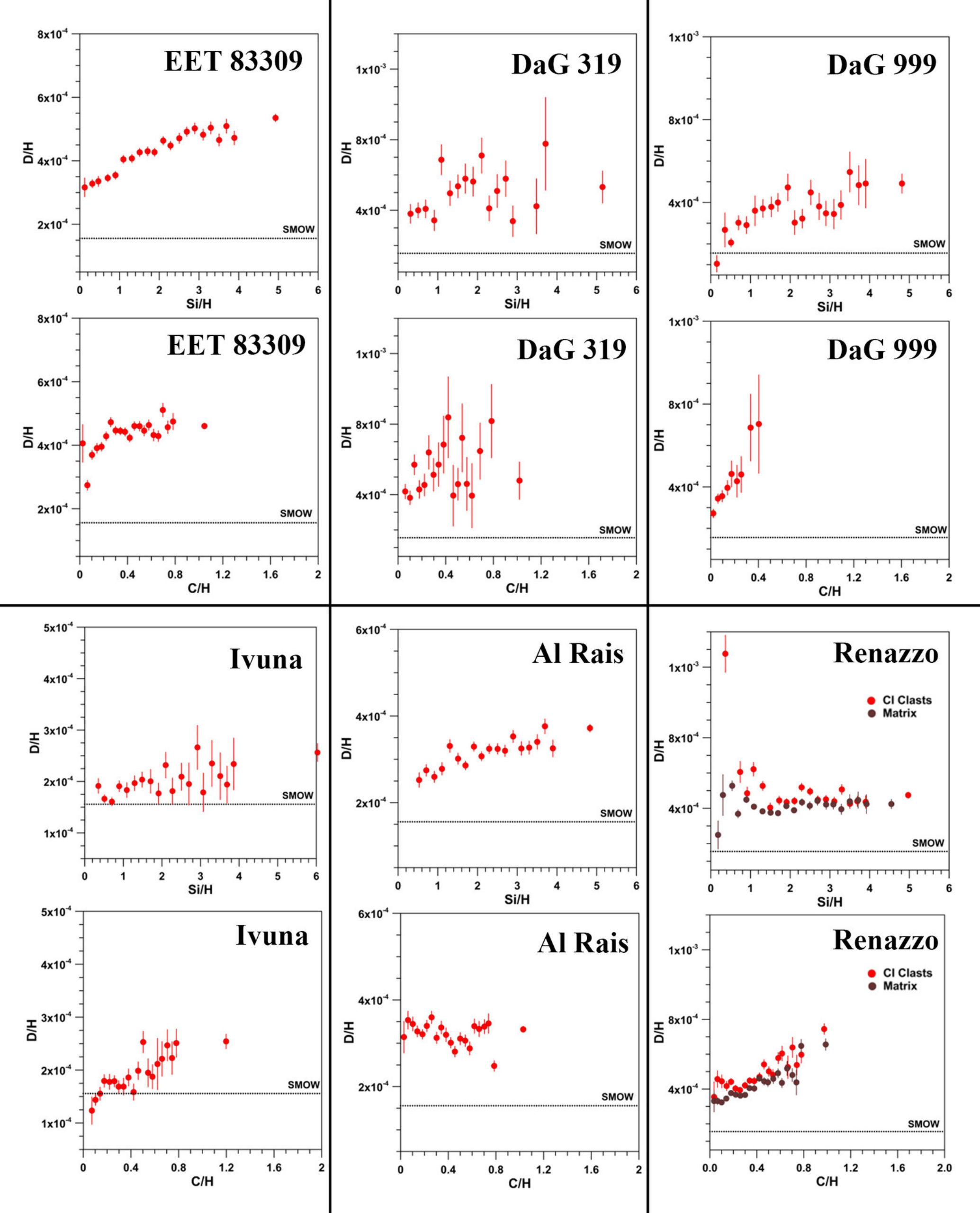
EET 83309
DaG 319
DaG 999
Ivuna
Al Rais
Renazzo
D/H
Si/H
C/H
SMOW
CI Clasts
Matrix
8x10⁻⁴
6x10⁻⁴
4x10⁻⁴
2x10⁻⁴
1x10⁻³
5x10⁻⁴
3x10⁻⁴
1x10⁻⁴
0 1 2 3 4 5 6
0 0.4 0.8 1.2 1.6 2
0.0 0.4 0.8 1.2 1.6 2.0

Saricicek
Al Rais
Bells
1H
12C
2H/1H
12C 14N
BSE
28Si
2494
1247
1
3381
1690
0
2.4E-003
1.2E-003
-2.2E-010
1805
902
0
550
275
0
3349
1674
0
4198
2099
0
2.1E-003
1.0E-003
-3.7E-010
2587
1293
0
424
212
0
3350
1675
1
2787
1393
0
9.3E-003
4.6E-003
-3.1E-010
2127
1063
0
287
144
1

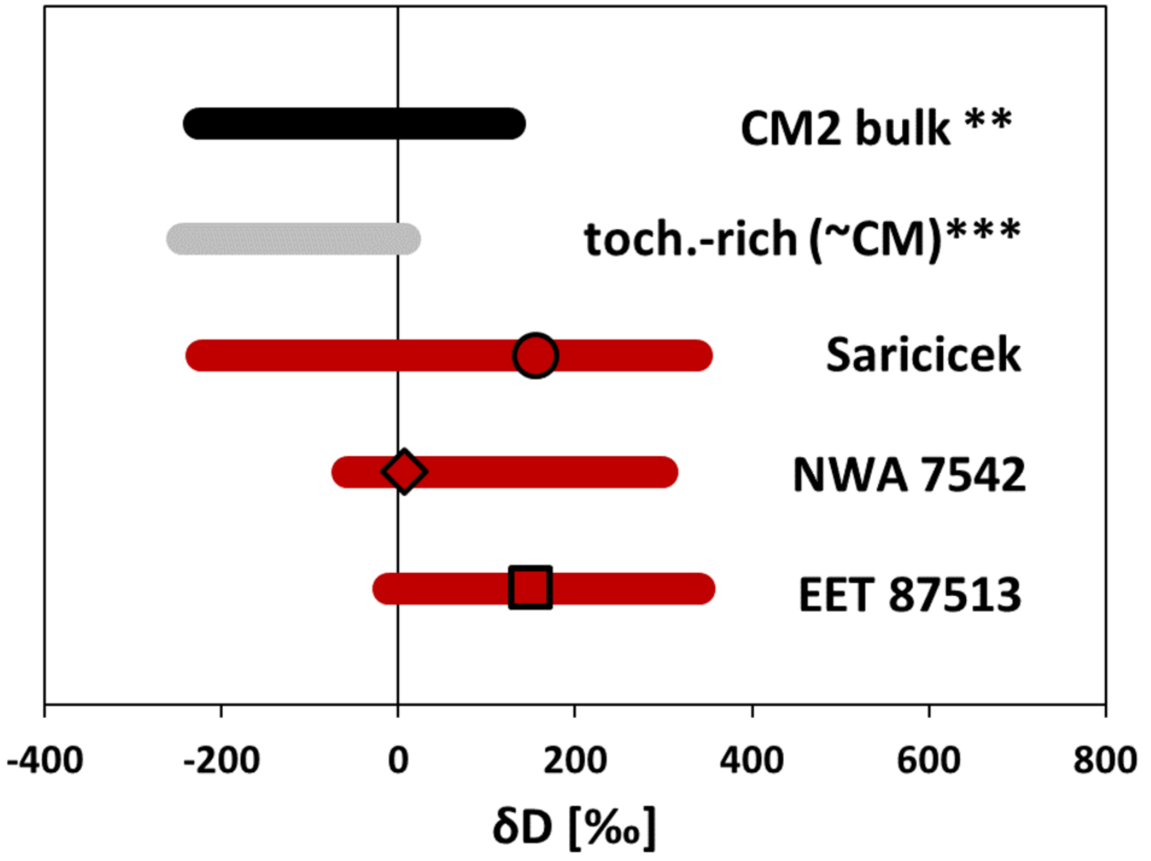
CM2 bulk **
toch.-rich (~CM)***
Saricicek
NWA 7542
EET 87513
-400
-200
0
200
400
600
800
δD [‰]

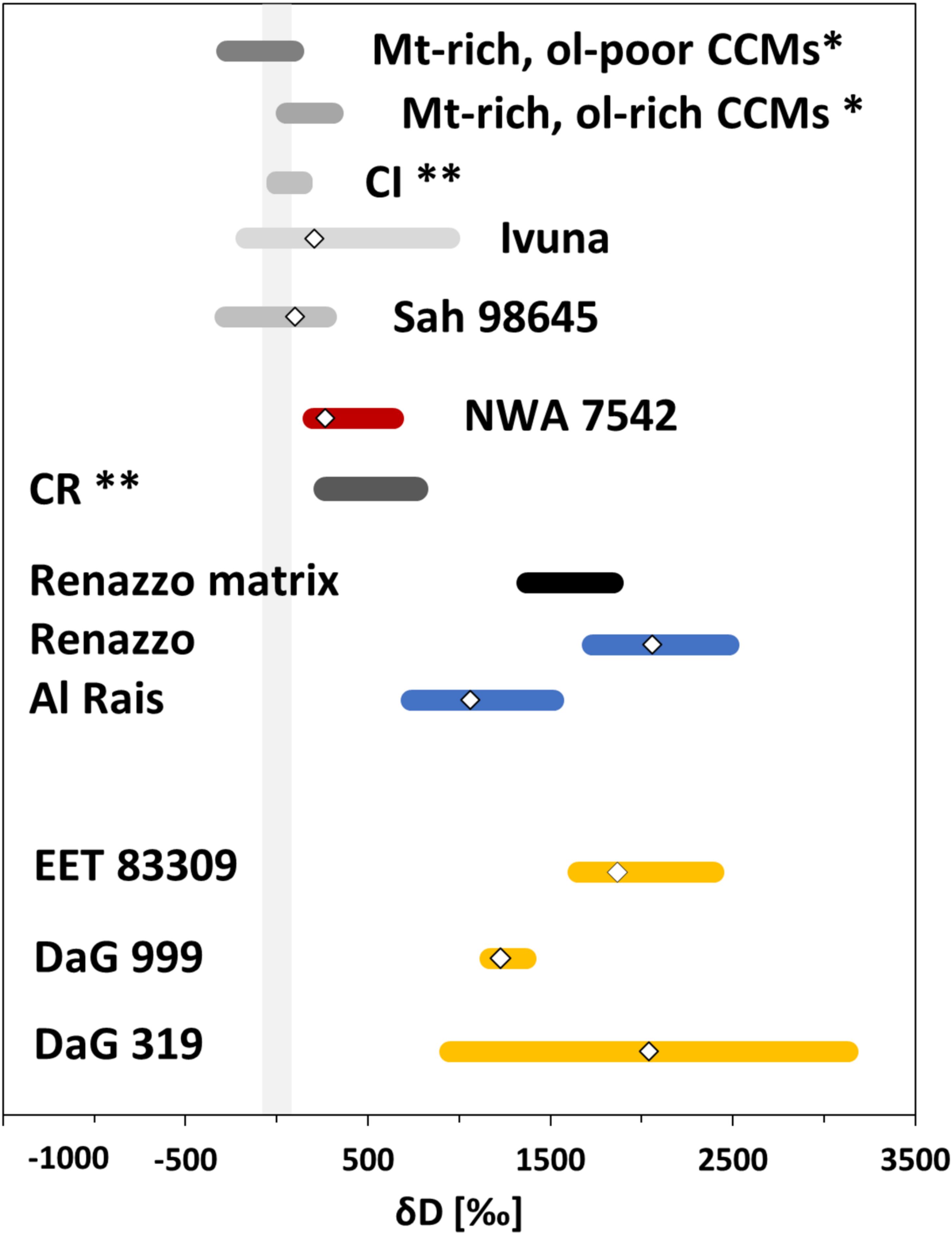
Mt-rich, ol-poor CCMs*
Mt-rich, ol-rich CCMs *
CI **
Ivuna
Sah 98645
NWA 7542
CR **
Renazzo matrix
Renazzo
Al Rais
EET 83309
DaG 999
DaG 319
-1000
-500
500
1500
2500
3500
δD [‰]

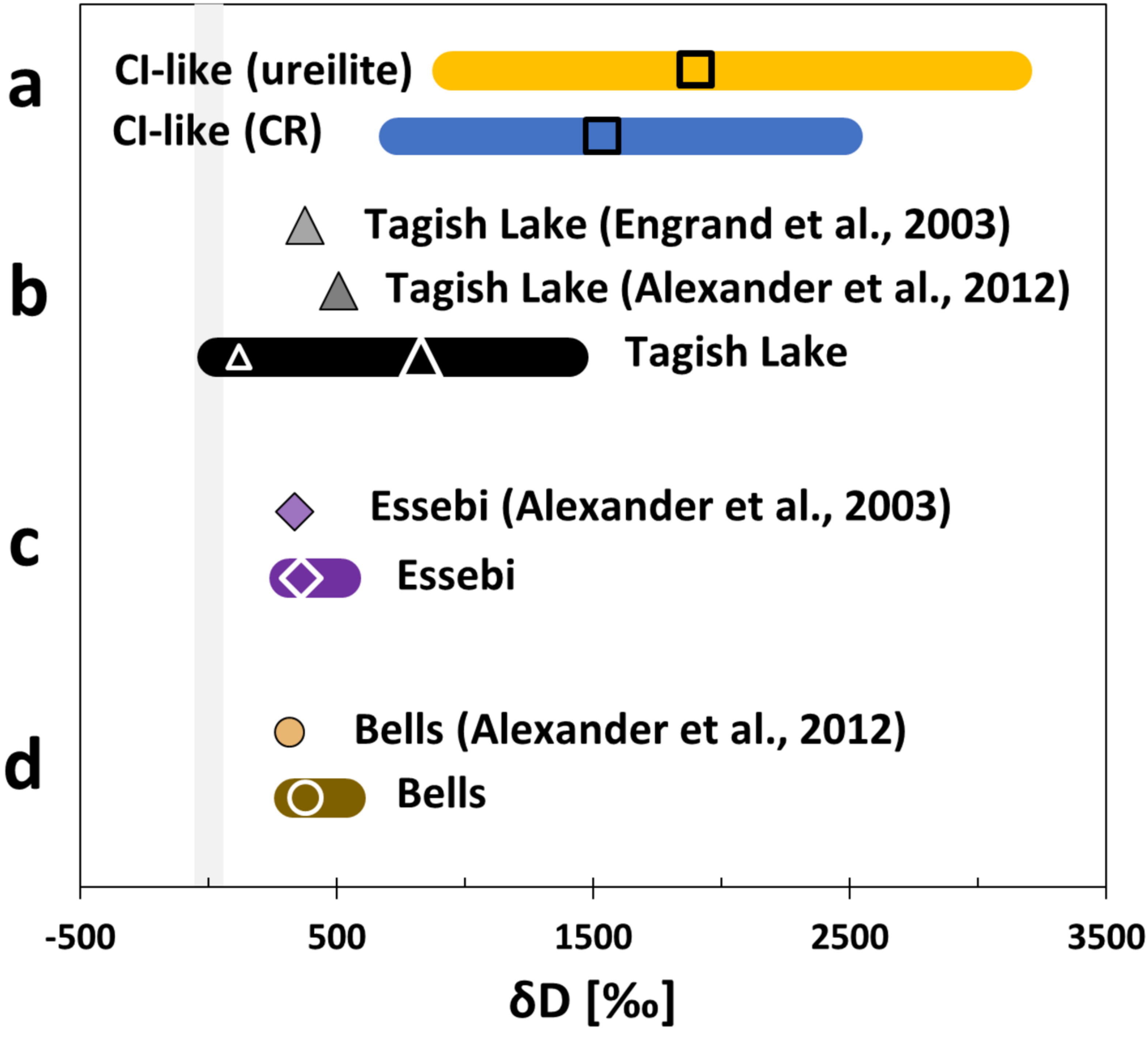
a
CI-like (ureilite)
CI-like (CR)
b
Tagish Lake (Engrand et al., 2003)
Tagish Lake (Alexander et al., 2012)
Tagish Lake
c
Essebi (Alexander et al., 2003)
Essebi
d
Bells (Alexander et al., 2012)
Bells
-500
500
1500
2500
3500
δD [‰]